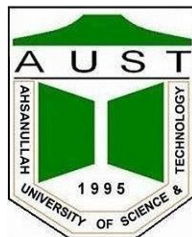


بسم الله الرحمن الرحيم

## **Effects of Lamina Stacking Sequence and Areal Weight (GSM) on the Mechanical Properties of S-Glass/Polyester Composites**

<b>Sajid Sadman</b>	<b>20200208153</b>
<b>Mahfuz Ahmed</b>	<b>20200208158</b>
<b>Raiyan Hossain</b>	<b>20200208116</b>



**DEPARTMENT OF MECHANICAL AND PRODUCTION ENGINEERING (MPE)**  
**AHSANULLAH UNIVERSITY OF SCIENCE AND TECHNOLOGY (AUST)**  
**DHAKA-1208, BANGLADESH**

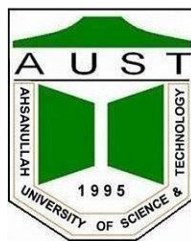
**June 2025**

# **Effects of Lamina Stacking Sequence and Areal Weight (GSM) on the Mechanical Properties of S-Glass/Polyester Composites**

By

<b>Sajid Sadman</b>	<b>20200208153</b>
<b>Mahfuz Ahmed</b>	<b>20200208158</b>
<b>Raiyan Hossain</b>	<b>20200208116</b>

A Thesis Submitted to the  
Department of Mechanical and Production Engineering,  
in Partial Fulfillment of the requirements for the Degree of  
BACHELOR OF SCIENCE IN MECHANICAL ENGINEERING



**DEPARTMENT OF MECHANICAL AND PRODUCTION ENGINEERING (MPE)**  
**AHSANULLAH UNIVERSITY OF SCIENCE AND TECHNOLOGY (AUST)**  
**DHAKA-1208, BANGLADESH**

**June 2025**

# **CERTIFICATE OF SUBMISSION**

---

The thesis entitled **Effects of Lamina Stacking Sequence and Areal Weight (GSM) on the Mechanical Properties of S-Glass/Polyester Composites** submitted by the following students has been accepted for partial fulfillment of the requirement for the degree of B.Sc. in Mechanical Engineering on [ ] as “on June,2025”

**Sajid Sadman**                           **20200208153**                           **Signature :** \_\_\_\_\_

**Mahfuz Ahmed**                           **20200208158**                           **Signature :** \_\_\_\_\_

**Raiyan Hossain**                           **20200208116**                           **Signature :** \_\_\_\_\_

**Supervisor Name:**

Dr Md. Kharshiduzzaman  
Associate Professor  
Department of Mechanical and Production Engineering  
Ahsanullah University of Science and Technology

**Signature :** \_\_\_\_\_

**External Name:**

Dr Fazlur Rahman  
Associate Professor  
Department of Mechanical and Production Engineering  
Ahsanullah University of Science and Technology

**Signature :** \_\_\_\_\_

**This work is dedicated to  
Our Loving Parents**

## **ACKNOWLEDGEMENT**

---

We would like to express our deepest gratitude to our respected supervisor, **Dr Md. Kharshiduzzaman**, for his unwavering support, insightful guidance, and constructive criticism throughout the course of our thesis titled [**Effects of Lamina Stacking Sequence and Areal Weight (GSM) on the Mechanical Properties of S-Glass/Polyester Composites**]. His profound expertise, meticulous attention to detail, and steadfast commitment to academic excellence have been instrumental in shaping the quality and direction of this research.

Dr Kharshiduzzaman's ability to challenge our perspectives while encouraging independent thought has greatly enriched our learning experience. His continuous encouragement, timely feedback, and valuable suggestions have not only enhanced the depth of our work but also helped us overcome numerous academic and practical challenges along the way.

This thesis would not have reached its present form without his consistent supervision and scholarly input. We are truly privileged to have had the opportunity to work under his mentorship.

# ABSTRACT

---

This study investigates the effects of lamina stacking sequence and areal weight (GSM) on the mechanical properties of S-glass fiber/polyester composite laminates. The primary objective is to evaluate the tensile and flexural behavior of quasi-isotropic laminates with various stacking sequences and GSM values. Laminates were fabricated using hand lay-up techniques with S-glass fiber reinforcement and polyester resin as the matrix material. Two distinct stacking sequences,  $[+60^\circ/0^\circ/-60^\circ]$  (anti-symmetric) and  $[0^\circ/+60^\circ/-60^\circ]$  (asymmetric), were selected to examine the influence of fiber orientation on mechanical performance. Additionally, composites with two areal weights, 200 GSM and 600 GSM, were evaluated to assess the impact of fiber volume fraction on the material's strength and stiffness. The research employs both experimental and analytical approaches. Classical Lamination Theory (CLT) was used for simulation to predict the laminate's stiffness, stress distribution, and strain behavior, while experimental tensile and bending tests were conducted according to ASTM standards. MATLAB was used to execute this Classical Lamination Theory (CLT) and Matplotlib was used for better visualization of results. The results indicate that the  $[+60^\circ/0^\circ/-60^\circ]$  laminate configuration provides superior bending and flexural strength at 200 GSM, while the  $[0^\circ/+60^\circ/-60^\circ]$  laminate exhibits improved tensile strength at 600 GSM. Further, the study demonstrates the significant influence of GSM on composite performance, where 200 GSM laminates excel in bending performance, while 600 GSM laminates show better tensile load-bearing capacity. This research contributes to optimizing composite laminate design for structural applications by identifying the ideal stacking sequence and GSM combination for enhanced mechanical performance.

# TABLE OF CONTENTS

---

<b>Topic</b>	<b>Page No.</b>		
<b>Certificate of Acceptance</b>	ii		
<b>Declaration of Candidate</b>	iii		
<b>Dedication</b>	iv		
<b>Acknowledgement</b>	v		
<b>Abstract</b>	vi		
<b>Table of Contents</b>	vii- viii		
<b>List of Tables</b>	ix		
<b>List of Figures</b>	x		
<b>List of Abbreviations</b>	xi		
<b>Nomenclature</b>	xii		
<b>Chapter</b>	<b>1</b>	<b>Introduction</b>	<b>01-03</b>
	1.1	Background	01
	1.2	Problem Statement	02
	1.3	Objectives	02
	1.4	Scope of Thesis	03

<b>Chapter</b>	<b>2</b>	<b>Literature Review</b>	<b>05-12</b>
	2.1	Tensile and Flexural Properties Evaluation	05
	2.2	Basalt/S-Glass Fiber Epoxy Mechanics	05
	2.3	Strength of Quasi Isotropic Glass Fiber	06
	2.4	Study Related to the influence of Stacking sequence	07
	2.5	Experimental Investigation of GFRP	08
	2.6	Mechanical Properties of Glass Fiber Reinforced	08
	2.7	CLT in Designing FRP Plates	09
	2.8	Stacking Sequence Effects on Laminates	09
	2.9	Research Gaps	10

<b>Chapter</b>	<b>3</b>	<b>Methodology</b>	<b>13-32</b>
	3.1	Overview	13
	3.2	Materials Used	14
	3.3	Laminate Configuration	18
	3.4	Fabrication process	21
	3.5	Experimental procedures	29

	3.5.1	Tensile Testing	29
	3.5.2	Bending Testing	30
3.6		Analytical and Simulation Approach	31
	3.6.1	Classical Lamination theory	32
	3.6.2	MATLAB Implementation	33
3.7		Validation and Comparison	33
3.8		Visual representation of the workflow	34
<b>Chapter</b>	<b>4</b>	<b>Results and Discussion</b>	<b>35-73</b>
	4.1	Experimental Analysis	35
	4.1.1	Bending Test	35
	4.1.2	Tensile test	41
	4.1.3	Test Result for 600 gsm	45
	4.1.4	Test result anti symmetric stacking sequence	48
	4.1.5	Test Result for Asymmetric stacking sequence	51
	4.2	Analytical Analysis	54
	4.2.1	Classical Laminate Theory Code	54
	4.2.2	Results Provided By the Code	57
	4.2.3	Code for Strain and Stress	57
	4.2.4:	Superimposed Graphs	67
	4.3	Validation	68
	4.4	Social Implications	70
	4.5	Sustainability and Environmental Implications	71

4.6	Limitations Of Thesis	74	
<b>Chapter</b>	<b>5</b>	<b>Conclusion and Recommendations</b>	<b>77-79</b>
5.1	Conclusion	77	
5.2	Recommendations	78	
<b>References</b>		<b>80-83</b>	
<b>Appendices</b>		<b>85-92</b>	
Appendix-A	Code for the Optimization Program	<b>85-92</b>	

## **LIST OF TABLES**

---

<b>Table No.</b>	<b>Table Title</b>	<b>Page No.</b>
Table 3.1	Material Properties	18
Table 4.2.1	Stress Distribution Values for Anti-symmetric	64
Table 4.2.2	Stress Distribution Values for Asymmetric	65

## LIST OF FIGURES

---

<b>Figure No.</b>	<b>Figure Title</b>	<b>Page No</b>
Fig 3.1	S-glass fiber strand with 1.5 mm width and 200 gsm	16
Fig 3.2	S-glass fiber strand with 2 mm width and 400 gsm	16
Fig 3.3	S-glass fiber strand with 3 mm width and 600 gsm	17
Fig 3.4	Custom alignment board marked	22
Fig 3.5	Application of polyester resin to S-glass fiber layers	23
Fig 3.6	Room temperature curing of the composite	24
Fig 3.7	Cutting of composite laminate into standard-sized specimens	25
Fig 3.8	Cutting of composite laminate specimens for tensile testing	26
Fig 3.9	Fabricated laminate specimen with anti-symmetric stacking	27
Fig 3.10	Fabricated laminate specimen with asymmetric stacking	27
Fig 3.11	Laminated composite specimen with anti-symmetric stacking	28
Fig 3.12	Composite laminate with asymmetric stacking sequence	28
Fig 3.13	Tensile testing of composite laminate specimen	30
Fig 3.15	Three-Point bending test of composite laminate	31
Fig 3.16	A detailed flowchart representing the step-by-step workflow	34
Fig 4.1.1	Bending strength of $[0^\circ/+60^\circ/-60^\circ]$ S-glass	35
Fig 4.1.2	Flexural modulus of S-glass laminate	36
Fig 4.1.3	Bending strength of S-glass laminate	36

<b>Figure No.</b>	<b>Figure Title</b>	<b>Page No</b>
Fig 4.1.4	Flexural modulus of anti-symmetric laminate	37
Fig 4.1.5	Stress - Strain curves of bending properties	37
Fig 4.1.6	Bending strength comparison of laminates	38
Fig 4.1.7	Flexural modulus comparison of laminates	38
Fig 4.1.8	Tensile strength of anti-symmetric laminate	40
Fig 4.1.9	Tensile modulus of anti-symmetric laminate	40
Fig 4.1.10	Tensile strength of asymmetric laminate	41
Fig 4.1.11	Tensile strength of asymmetric S-glass laminate	41
Fig 4.1.11	Tensile strength comparison of S-glass laminates	41
Fig 4.1.12	Stress - Strain curves of tensile properties	42
Fig 4.1.13	Tensile Strength comparison	43
Fig 4.1.14	Tensile modulus comparison of S-glass laminates	43
Fig 4.1.15	Bending strength comparison of 600 gsm laminates	45
Fig 4.1.16	Flexural modulus comparison of 600 gsm laminates	45
Fig 4.1.17	Tensile strength comparison of 600 gsm laminates	47
Fig 4.1.18	Tensile modulus comparison of 600 gsm laminates	47
Fig 4.1.19	Bending Strength Comparison: 200 vs 600 GSM	48
Fig 4.1.20	Flexural Modulus: 200 vs 600 GSM	49
Fig 4.1.21	Tensile Strength: 200 vs 600 GSM	49
Fig 4.1.22	Tensile Modulus: 200 vs 600 GSM	50
Fig 4.1.23	Bending Strength: 200 vs 600 GSM	51

Fig 4.1.24	Flexural Modulus: 200 vs 600 GSM	52
Fig 4.1.25	Tensile Strength: 200 vs 600 GSM	52
Fig 4.1.26	Tensile Modulus: 200 vs 600 GSM	53

<b>Figure No.</b>	<b>Figure Title</b>	<b>Page No</b>
Fig 4.2.1	MATLAB Command Window	57
Fig 4.2.2	Mid-plane Strain Distribution Anti-Symmetric	62
Fig 4.2.3	Mid-plane Strain Distribution Asymmetric	63
Fig 4.2.4	Stress Distribution Anti -Symmetric	64
Fig 4.2.5	Stress Distribution Asymmetric	65
Fig 4.2.6	Super Imposed Strain Components	67
Fig 4.2.7	Super Imposed Stress Components	68
Fig 4.3.1	Validation for A Matrix	68
Fig 4.3.2	Validation for B&D Matrices	68
Fig 4.3.3	Validation for Strain Distribution	68
Fig 4.3.4	Validation for Stress Distribution	68

## NOMENCLATURE

---

Symbol	Description
$f$	Friction factor
$a_g$	Acceleration due to gravity
VCC	Voltage Common Collector
$V_f$ and $V_m$	Volume fraction of fiber and matrix
$E_f$ and $E_m$	Constituent properties, Elastic modulus of fiber and matrix
$\nu_f$ and $\nu_m$	Constituent properties, Poisson's ratio of fiber and matrix.
$G_f$ and $G_m$	Constituent properties, Shear modulus of fiber and matrix.
$E_1$ and $E_2$	Lamina properties, Elastic modulus along longitudinal and transverse direction. Moment load per unit length, acting on laminate.
$G_{12}$	Mid-plane strain or stretching of laminate.
$\nu_{12}$	The curvature of the laminate.
$Q$	Stress and strain acting on laminate.
$S$	Lamina property, Transformed stiffness in global directions.
$t_k$	Lamina property, Lamina (ply) thickness.

$Z_b$	Lamina property, Mid-plane to mid-plane distance of a lamina.
A	Laminate property, In-plane extension stiffness.
D	Laminate property, In-plane bending stiffness.
$\infty$	Laminate property, the inverse of in-plane stiffness, A.
$\delta$	Laminate property, inverse of bending stiffness, D.
t	Laminate (or plate) thickness.
N	In-plane extension load per unit length, acting on laminate.
M	Moment load per unit length, acting on laminate.
$\varepsilon_{10}$	Mid-plane strain or stretching of laminate.
K	The curvature of the laminate.
$\sigma$ and $\varepsilon$	Stress and strain acting on laminate.



# Chapter 1

## INTRODUCTION

---

### 1.1 Background

Composite materials have increasingly become essential in modern engineering due to their high strength-to-weight ratios, corrosion resistance, and customizable mechanical properties. Among the various types of composite materials, fiber-reinforced polymer (FRP) composites have shown great promise in structural applications ranging from aerospace to automotive and civil engineering [9].

S-glass fiber, a high-strength variant of E-glass, offers enhanced tensile properties and thermal resistance, making it a suitable reinforcement for high-performance composites. Polyester resin, known for its ease of processing and cost-effectiveness, is often used as the matrix material in such applications [10]. The mechanical performance of these composites is highly dependent on their stacking sequence, the orientation of fiber plies, and the fabric areal weight (gsm).

Quasi-isotropic laminates, particularly with varying degrees of symmetry and asymmetry in stacking sequences, exhibit different responses under mechanical loads. Understanding the tensile and flexural behavior of these configurations is crucial for optimizing laminate design and ensuring structural integrity in real-world applications [11].

## **1.2 Problem Statement**

Although extensive research has been conducted on composite laminates, limited studies address the comparative performance of symmetric, anti-symmetric, and asymmetric quasi-isotropic laminates fabricated with different fiber areal weights. The influence of stacking sequence symmetry and gsm variation on tensile and flexural behavior remains insufficiently explored, particularly in composites reinforced with S-glass fiber and polyester resin. This research aims to fill this gap by experimentally and analytically analyzing and comparing various laminate configurations to identify the most efficient design for load-bearing applications.

## **1.3 Objectives**

The main objectives of this research are:

- To fabricate quasi-isotropic composite laminates using S-glass fiber and polyester resin with varying stacking sequences and gsm.
- To evaluate the mechanical performance of anti-symmetric  $[+60^\circ / 0^\circ / -60^\circ]$  and asymmetric  $[0^\circ / \pm 60^\circ]$  laminates with 200 gsm and 600 gsm.
- To compare the mechanical properties of these laminates in order to determine the optimal stacking sequence and gsm combination.
- To compute the distribution of stress over laminate thickness using MATLAB

- To compute the strains and distribution of strains over laminate thickness using MATLAB.
- To provide insights and recommendations for future applications of such composite laminates in engineering structures.

## 1.4 Scope of the Thesis

The study is specifically limited to quasi-isotropic laminate configurations using two stacking sequences—anti-symmetric  $[+60^\circ/0^\circ/-60^\circ]$  and asymmetric  $[0^\circ/+60^\circ/-60^\circ]$ —and two areal weights—200 GSM and 600 GSM. These constraints allow for a controlled examination of the role played by fiber orientation and fiber volume fraction in determining the mechanical response of the composite materials.

The **experimental component** of the study includes tensile and flexural (bending) testing performed in accordance with ASTM standards. These tests provide empirical data on tensile strength, flexural strength, and corresponding modulus values, enabling a comparative assessment of how different stacking patterns and GSM values influence material stiffness, ductility, and load-bearing capacity. The mechanical performance metrics obtained offer practical insights into which laminate configurations are most suitable for stiffness-dominated or strength-dominated applications.

Complementing the experimental approach, a **Classical Lamination Theory (CLT)** framework is implemented via MATLAB to simulate stress and strain distributions through the laminate thickness. The simulation produces stiffness matrices ([A], [B], and [D]), mid-plane strain and curvature profiles, and detailed ply-by-ply stress-strain distributions. These analytical results offer a theoretical basis for understanding internal force interactions, bending-stretching coupling, and anisotropic behavior, particularly in asymmetric laminates. The correlation between experimental results and analytical predictions validates the effectiveness of CLT in modeling composite behavior and informs future optimization of laminate design.

In summary, the scope of this study is confined to evaluating the static mechanical properties of S-glass/polyester laminates under controlled laboratory conditions. The findings are applicable to the design and development of lightweight structural components in industries such as aerospace, automotive, and civil engineering, where material efficiency and directional performance are critical.

# **Chapter 2**

## **LITERATURE REVIEW**

---

### **2.1 Evaluation of Tensile and Flexural Properties of Woven Glass Fiber Reinforced Polyester Composites.**

The study examines the mechanical properties of woven glass fiber-reinforced polyester composites, with a specific focus on tensile strength, flexural strength, and the influence of fiber orientation. The paper examines the impact of various fiber layup configurations on the composite's performance, providing a comprehensive understanding of how woven glass fibers improve the mechanical properties of polyester composites. The study found that woven glass fibers significantly improve the tensile strength of polyester composites [3]. The orientation of fibers plays a crucial role in optimizing the tensile properties, with specific reference to bidirectional woven fibers that improve stress distribution. Similar improvements were observed in the flexural strength, with the fiber orientation being key to the composite's bending resistance. The study showed that the performance of woven glass fiber composites could be tailored by adjusting the fiber angles, particularly those in the 0° and 90° orientations.

### **2.2 Mechanical Investigation of Basalt/S-Glass Fiber Reinforced Epoxy Composites.**

The paper investigates the mechanical properties of basalt and S-glass fiber-reinforced epoxy composites. The research primarily focuses on tensile strength, flexural strength, and impact resistance of the composites. The authors highlight that S-glass fibers exhibit superior mechanical properties compared to basalt fibers, such as increased strength and stiffness. The study is particularly concerned with understanding how these fibers, when combined with epoxy resin, perform under stress. The epoxy resin matrix is chosen for its excellent bonding properties, which enhance the overall load-bearing capacity and durability of the composite [4].

The results from this paper provide valuable data that could help optimize the use of S-glass fibers in engineering applications requiring high mechanical performance. The study also compares the performance of S-glass fibers with basalt fibers, offering insight into how different types of fibers influence the composite material's behavior.

### **2.3 Strength of Quasi-Isotropic Glass Fiber Laminate.**

This thesis focuses on the mechanical properties of quasi-isotropic glass fiber laminates, specifically analyzing bending modulus and shear modulus. A quasi-isotropic laminate is designed to exhibit isotropic behavior, meaning the laminate will have similar properties in all directions. The paper emphasizes the importance of laminate stacking sequences (such as  $[+45^\circ/-45^\circ]$  or  $[0^\circ/90^\circ]$ ), and their effect on the strength, bending stiffness, and shear performance of the composite. Various tests, including tensile, flexural, and shear strength testing, are used to evaluate the material's behavior under different loading conditions [6].

The study provides theoretical background on laminate theory, followed by experimental analysis to validate theoretical predictions. The findings reveal how the fiber orientation significantly influences mechanical properties and how optimized stacking sequences can improve the structural efficiency of composite materials in practical applications.

## **2.4 Study Related to the Influence of Stacking Sequence on Stress and Strain in Quasi-Isotropic Laminates.**

This research paper focuses on composite materials designed for quasi-isotropic laminates, with a particular emphasis on the mechanical properties of these materials when subjected to various loading conditions. It presents theoretical and experimental data on different stacking sequences, specifically examining configurations such as  $[+60^\circ/0^\circ/-60^\circ]$  and  $[0^\circ/\pm60^\circ]$  for their impact on the overall laminate performance [7].

The study analyzes the strength, stiffness, and failure characteristics of laminates with different fiber orientations, evaluating how these factors contribute to the laminate's ability to resist tensile, flexural, and shear forces. A significant focus of the research is the effect of fiber orientation on the failure modes, including delamination and fiber breakage, and how these failure mechanisms vary based on the laminate configuration.

Additionally, the paper discusses the role of fiber-matrix interaction, emphasizing the importance of good bonding between the fiber and matrix to ensure the laminate's structural integrity. The research also compares different layering techniques for fiber-reinforced laminates, drawing

conclusions on the best configurations for achieving balanced mechanical properties in composite structures.

## **2.5 Experimental Investigation on Mechanical Behaviour of GFRP Laminates with Different Stacking Sequences.**

This study investigates the mechanical properties of glass fiber-reinforced polymer (GFRP) laminates fabricated with different stacking sequences. Using tensile, flexural, and impact testing methods, the authors analyze how the orientation of plies (e.g.,  $0^\circ$ ,  $90^\circ$ ,  $\pm 45^\circ$ ) affects strength and stiffness. Results show that laminates with mixed orientations provide improved impact resistance and moderate tensile and flexural strengths, emphasizing the critical role of fiber direction in composite performance [1].

## **2.6 Mechanical Properties of Glass Fiber Reinforced Polyester Composites.**

This research investigates how the mechanical properties of GFRP composites are influenced by fiber orientation and layering. Using tensile and flexural tests, the study compares various layups of glass fiber in a polyester matrix. Results highlight that aligned fibers yield better tensile strength, while multi-directional orientations enhance flexural performance [2]. The study demonstrates the sensitivity of composite behavior to structural design and material selection, contributing to optimized composite use in load-bearing applications.

## **2.7 Classical Laminate Theory (CLT) and Its Use for Designing and Manufacturing of FRP Plates.**

Bhavik Panchal (2021) presents a comprehensive and accessible explanation of the Classical Laminate Theory (CLT) and its application in the design and manufacturing of fiber-reinforced polymer (FRP) plates. The paper outlines the fundamental assumptions of CLT, such as thin laminate behavior, perfect bonding between layers, linear elasticity, and the neglect of transverse shear deformation. It emphasizes how the stress-strain relationship within each ply is defined using a stiffness matrix  $[Q][Q][Q]$ , which is then transformed  $[Q'][Q'][Q']$  based on the fiber orientation. The paper also details how the overall stiffness of a laminate is represented through the ABD matrix, where the  $[A]$  matrix defines in-plane stiffness,  $[B]$  represents bending-extension coupling, and  $[D]$  describes bending stiffness. Panchal derives and explains the global CLT equation that relates in-plane loads and moments to mid-plane strains and curvatures [5]. The study demonstrates how CLT can be used to predict laminate behavior under mechanical loads and optimize the stacking sequence for improved structural performance. While it highlights CLT's effectiveness in laminate design, it also notes limitations, such as its inaccuracy for thick laminates or for predicting out-of-plane stresses.

## **2.8 ASTM D638-22 – Standard Test Method for Tensile Properties of Plastics.**

ASTM D638-22 is a standardized method developed by ASTM International for determining the tensile properties of plastics, including tensile strength, yield strength, elongation, and modulus of elasticity. It is widely used in both industry and research to characterize the mechanical performance of rigid and semi-rigid polymers. The standard defines five specimen types (Types I–V), with Type I being the most common. It outlines specific testing conditions such as

temperature ( $23 \pm 2$  °C), humidity ( $50 \pm 10\%$ ), and crosshead speeds, which vary depending on material properties. Testing involves pulling a specimen until failure while recording the stress-strain response, typically using an extensometer for accurate strain measurements. ASTM D638-22 is commonly cited in studies on material development, composite reinforcement, and 3D-printed polymers, providing a consistent method for comparing mechanical behavior. It also includes an optional measurement of Poisson's ratio, useful for advanced modeling [8].

## 2.9 Research Gaps

Despite significant advancements in the study of composite materials, several gaps remain, particularly in the context of S-glass fiber-reinforced polyester composites used in quasi-isotropic laminates. One of the key gaps is the limited research specifically focused on the combination of S-glass fibers with polyester resin in quasi-isotropic laminate configurations. While S-glass fibers are known for their superior mechanical properties, there is a lack of comprehensive studies that explore their performance in this specific resin system. This leaves a gap in understanding how S-glass and polyester resin behave together, especially in more complex laminate designs.

Another gap lies in the insufficient exploration of stacking sequences in composite laminates. Although various configurations have been studied, there is limited research comparing the mechanical properties of laminates with the specific stacking sequences [+60°/0°/-60°] and [0°/ $\pm 60^\circ$ ]. These sequences are important as they affect the laminate's stiffness, strength, and overall performance [4]. Further investigation into how these particular sequences influence the

composite material is necessary for more optimized designs, especially in engineering applications where precision in mechanical performance is crucial.

Furthermore, the impact of fiber weight in composite laminates remains underexplored. Most studies focus on a single fiber grammage, but the mechanical properties of composites made with fibers of different grammages, such as 200 gsm and 600 gsm, have not been adequately compared [5]. Understanding how fiber weight affects tensile strength, bending modulus, and the failure behavior of the laminates is essential, especially when designing composites for high-performance applications.

Additionally, there is a lack of research on hybrid composites made from different fiber weights, such as 200 gsm and 600 gsm. Hybrid composites are particularly relevant in applications where the cost of materials and desired mechanical properties need to be balanced. The influence of varying fiber weights on the performance and cost-effectiveness of the laminates is an area that requires more detailed study.

This study will address these research gaps by focusing on the performance of S-glass fibers with polyester resin in quasi-isotropic laminate configurations. We will investigate the mechanical properties of laminates using two distinct stacking sequences,  $[+60^\circ/0^\circ/-60^\circ]$  and  $[0^\circ/\pm60^\circ]$ , to compare how these sequences influence laminate strength and stiffness.

In addition, we will explore the impact of fiber weight by comparing laminates made from 200 gsm and 600 gsm S-glass fibers. This will allow for a deeper understanding of how variations in fiber grammage affect the mechanical behavior of the composite material. Finally, our work will contribute to the field of hybrid laminates by studying the combination of 200 gsm and 600 gsm

fibers in the same laminate, shedding light on how different fiber weights can be optimized for cost-effective and high-performance applications.

# Chapter 3

## METHODOLOGY

---

### 3.1 OVERVIEW

The purpose of this study is to assess the effect of various stacking sequences regarding mechanical performance of quasi-isotropic composite laminates. The emphasis here is on the arrangement of fiber tracking whereby stress distribution, strain response and flexural behaviour under loading are of primary concern. In this regard, composite laminates have been prepared by incorporating S-glass fiber and polyester resin as the matrix material [12]. These materials are widely used in aerospace, automotive, marine, and sporting industries due to their excellent strength-to-weight ratio, corrosion resistance, and ease of processing.

To systematically evaluate the effect of stacking sequence, three distinct types of quasi-isotropic laminates were prepared: an anti-symmetric laminate  $[+60^\circ/0^\circ/-60^\circ]$ , and an asymmetric laminate  $[0^\circ/\pm60^\circ]$ . Each configuration was tested with varying areal weights (200 gsm and 600 gsm) to observe the influence of fiber volume fraction on mechanical properties [13].

The research methodology integrates both analytical modeling and experimental testing. The analytical part employs Classical Lamination Theory (CLT) implemented in MATLAB to predict in-plane stiffness matrices, stress distributions, and mid-plane strain responses for each laminate

configuration [25]. These theoretical results provide a foundational understanding of laminate mechanics and guide the interpretation of experimental outcomes.

The experimental phase includes mechanical characterization through tensile and flexural (bending) tests, following standardized testing procedures (ASTM D638 and ASTM D790, respectively). Laminates were fabricated using the hand lay-up technique, ensuring controlled stacking orientation and resin application. After curing, the specimens were precisely cut and tested using a Universal Testing Machine (UTM) to measure parameters such as tensile strength, Young's modulus, flexural strength, and flexural modulus [14].

A comparison of analytical and experimental results leads to the identification of the stacking sequence with the best mechanical performance. The comparative assessment performed in this study provides insights that can help in the design and optimizing composite laminates for applications where both directional stiffness and strength are important factors in load bearing capacities.

### **3.2 Materials Used**

A high-performance fiber reinforcement and a thermosetting polymer matrix were used to make the composite laminates studied here. The materials were chosen considering mechanical performance, availability, and compatibility to structural applications.

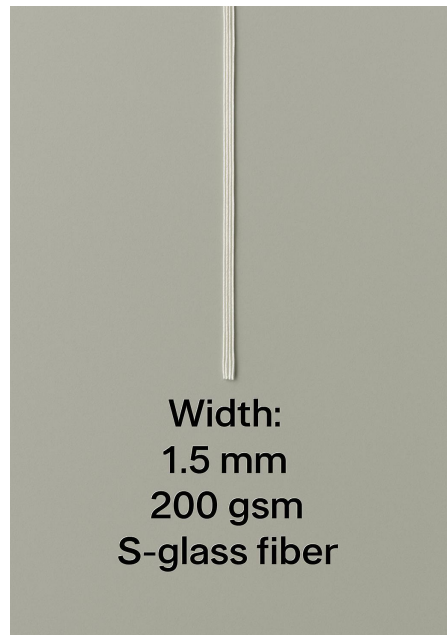
**The laminates were made using:**

- **Fiber reinforcement: S-glass fiber**

**S-glass (structural glass)** fiber was used as the reinforcing material in all laminate configurations. Compared to the more commonly used E-glass, S-glass fibers offer superior tensile strength, higher modulus of elasticity, and better resistance to fatigue and high temperatures [15]. These fibers are made from a special formulation of **alumino-silicate glass** and are widely used in aerospace and high-performance structural applications due to their enhanced mechanical and thermal properties.

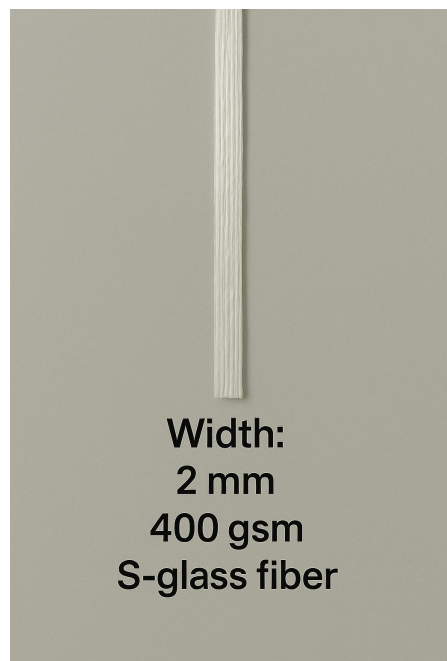
**Key Properties of S-glass Fiber:**

- High tensile strength and stiffness.
- Good impact resistance.
- Excellent fatigue durability [16].
- Areal densities used: 200 gsm and 600 gsm (grams per square meter).



**Width:**  
1.5 mm  
200 gsm  
S-glass fiber

**Figure 3.1:** S-glass fiber strand with 1.5 mm width and 200 gsm.



**Width:**  
2 mm  
400 gsm  
S-glass fiber

**Figure 3.2:** S-glass fiber strand with 2 mm width and 400 gsm.



**Figure 3.3:** S-glass fiber strand with 3 mm width and 600 gsm.

- **Matrix: Polyester resin**

The matrix used for binding the fibers was an unsaturated polyester resin, a thermosetting polymer widely recognized for its ease of processing, cost-effectiveness, and good mechanical strength [17]. Polyester resin serves multiple roles in the composite structure:

- It holds the fibers in place and transfers stress between them.
- Provides shape and structural integrity.
- Protects the fibers from environmental damage and wear.

To initiate the curing process, Methyl Ethyl Ketone Peroxide (MEKP) was used as a catalyst. The resin and catalyst were mixed in an appropriate ratio (typically around 1–2% by weight) and applied uniformly during lay-up [18].

Material properties used for simulation and validation: [7]

Properties	S-Glass Fiber	Polyester resin
Young's Modulus, E (GPa)	85.5	4
Poisson's Ratio, $\nu$	0.22	0.39
Shear Modulus, G (GPa)	26.72	1.44
Density, $\rho$ (kg/m <sup>3</sup> )	2500	1200

**Table 3.1:** Material Properties

### 3.3 Laminate Configurations

In this study, two quasi-isotropic laminate configurations were selected to examine how variations in stacking sequence influence mechanical performance, particularly stress and strain distributions and flexural behavior. Both laminates use identical materials, fiber orientations, ply thicknesses, and number of plies to ensure that the only variable is the order in which the layers are stacked.

A **quasi-isotropic laminate** is designed to mimic isotropic in-plane behavior by using multiple plies oriented at specific angles. This allows the laminate to exhibit uniform stiffness in all in-plane directions. According to Classical Lamination Theory (CLT), a laminate exhibits quasi-isotropic behavior in its extensional stiffness matrix  $[A][A][A]$  if the fiber orientations are arranged to satisfy:

- $A_{11}=A_{22}$   $A_{-11}=A_{-22}$
- $A_{16}=A_{26}=0$   $A_{-16}=A_{-26}=0$
- $A_{66}=A_{11}-A_{12}^2$   $A_{-66}=\frac{A_{11}-A_{12}}{2}$   $A_{66}=2A_{11}-A_{12}$

These conditions are achieved using symmetric or carefully chosen asymmetric stacking sequences with angles such as  $0^\circ$ ,  $\pm 45^\circ$ ,  $\pm 60^\circ$ , and  $90^\circ$ .

- **Selected Configurations**

### 1. Anti-Symmetric Quasi-Isotropic Laminate

- Stacking sequence:**  $[+60^\circ/0^\circ/-60^\circ]$ .
- Type:** Anti-symmetric.
- In this configuration, the laminate is arranged such that the fiber orientations are mirrored in sign with respect to the mid-plane but not mirrored in position. The anti-symmetric layout can introduce coupling between bending and twisting (nonzero [B] matrix), making it ideal for studying shear-bending interactions. However, the overall in-plane stiffness matrix [A] still retains quasi-isotropic characteristics due to the balanced angular distribution [7].

## 2. Asymmetric Quasi-Isotropic Laminate

- **Stacking sequence:**  $[\pm 60^\circ/0^\circ]$ .
- **Type:** Asymmetric.
- This configuration has no symmetry about the mid-plane, and while it maintains the same fiber orientation angles and ply count, the stacking order changes the laminate's response to out-of-plane loads. Asymmetric laminates generally exhibit strong bending-stretching coupling and warping, which are manifested as nonzero terms in the [B] and [D] matrices. This makes them a good candidate for assessing the influence of stacking on flexural behavior [7].

### Common Characteristics of Both Laminates[7]

- **Number of plies:** 3
- **Ply thickness:** 0.4 mm (total laminate thickness = 1.2 mm).
- **Fiber orientations:**  $-60^\circ, 0^\circ, +60^\circ$
- **Material system:** S-glass fiber (reinforcement) and polyester resin (matrix).

By keeping the ply count, orientations, and material properties constant, the study isolates the effect of stacking sequence alone on the laminate's mechanical response. This approach aligns with the requirements of quasi-isotropic behavior and allows direct comparison between configurations using both analytical and experimental results.

### **3.4 Fabrication Process**

The fabrication of composite laminates in this study was carried out using standard techniques suitable for fiber-reinforced polymer composites. Special care was taken to ensure uniform fiber distribution, correct stacking sequence, and proper resin impregnation to achieve high-quality laminates.

- **Base alignment board with angular guides:** To ensure accurate fiber orientation during the hand lay-up process, a custom alignment board was prepared and used as the base platform. This board was marked with angular reference lines corresponding to  $+60^\circ$ ,  $0^\circ$ , and  $-60^\circ$  orientations, which are the key angles used in the stacking sequences of the quasi-isotropic laminates. The reference lines were drawn with a 1 cm spacing between each long marking, providing a visual guide for precise alignment of the S-glass fiber layers during lay-up. This setup ensured consistency across all specimens and minimized angular misalignment, which is critical for maintaining the integrity of the designed stacking sequence and for achieving reliable mechanical test results.



**Figure 3.4:** Custom alignment board marked with  $+60^\circ$ ,  $0^\circ$ , and  $-60^\circ$  orientation lines at 10 mm intervals, used for accurate fiber placement during composite lay-up.

- **Method:** Hand lay-up [23]

The hand lay-up technique was employed for laminate fabrication. This is a widely used method for producing composite structures due to its simplicity, low cost, and suitability for small-scale production and experimental research.

- In this method, pre-cut layers of S-glass fiber were placed manually on a flat mold surface according to the designed stacking sequence.
- Polyester resin, mixed with Methyl Ethyl Ketone Peroxide (MEKP) as a curing agent, was applied uniformly between each layer to ensure proper wetting and bonding. [24]

- A brush was used to remove air bubbles and distribute the resin evenly, ensuring a void-free and compact laminate.



**Figure 3.5:** Application of polyester resin to S-glass fiber layers using a brush during the hand lay-up process.

- **Curing:** After the hand lay-up process, the laminates were left to cure at ambient room temperature without the application of any external pressure. The curing occurred under atmospheric conditions to allow the polyester resin to undergo polymerization and harden over time.[19] This natural curing process ensures that the matrix fully sets and bonds the

fiber layers together. Adequate care was taken during lay-up to avoid resin pooling or voids, ensuring uniform thickness and proper fiber wetting without needing additional compression.



**Figure 3.6:** Room temperature curing of the composite laminate without external pressure, following the hand lay-up process.

- **Post-curing:** To further enhance the mechanical properties of the composite. The laminates were allowed to post-cure for 24 hours at room temperature after initial curing. This process improves cross-linking in the polyester matrix, thereby increasing its

thermal and mechanical stability. [26]

- **Cutting:** To ensure consistency, repeatability, and comparability of mechanical test results, the composite specimens were prepared and tested following recognized ASTM (American Society for Testing and Materials) standards. Specifically, **ASTM D638** was followed for tensile testing and **ASTM D790** for flexural (bending) testing.[8]



**Figure 3.7:** Cutting of composite laminate into standard-sized specimens for flexural testing in accordance with ASTM D790.



**Figure 3.8:** Cutting of composite laminate specimens for tensile testing as per ASTM D638 standard.

- **Specimen Preparation for Testing [8]**

1. [+60/0/-60] using 200 gsm S-glass fiber (for both tensile and bending tests).



**Figure 3.9:** Fabricated laminate specimen with anti-symmetric stacking sequence  
[+60/0/-60] using 200 gsm S-glass fiber.

2. [0/+60/-60] using 200 gsm S-glass fiber (for both tensile and bending tests).



**Figure 3.10:** Fabricated laminate specimen with asymmetric stacking sequence  
[0/+60/-60] using 200 gsm S-glass fiber.

3.  $[+60/0/-60]$  using 600 gsm S-glass fiber (for both tensile and bending tests).



**Figure 3.11:** Laminated composite specimen with anti-symmetric stacking sequence  $[+60/0/-60]$  using 600 gsm S-glass fiber.

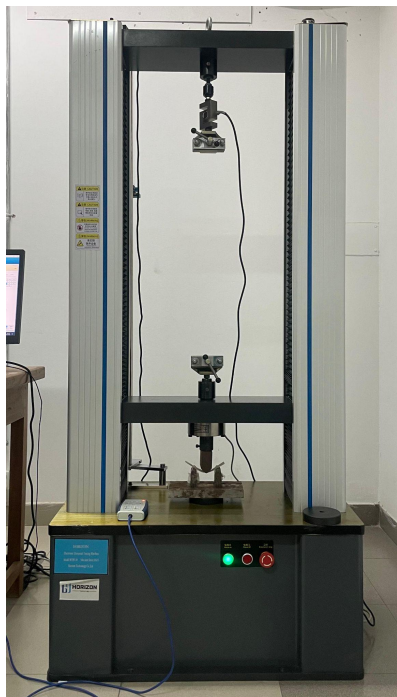
4.  $[0/+60/-60]$  using 600 gsm S-glass fiber (for both tensile and bending tests).



**Figure 3.12:** Composite laminate with asymmetric stacking sequence  $[0/+60/-60]$  using 600 gsm S-glass fiber.

### 3.5 Experimental Procedures

A **Universal Testing Machine (UTM)** was used to perform both tensile and three-point bending (flexural) tests on S-glass fiber-reinforced polyester composite specimens. [20] The machine includes a load cell, grips for tensile testing, and fixtures for flexural loading, and is connected to FastTest software for real-time data acquisition and stress–strain analysis.



#### 3.5.1 Tensile Testing [27]

- **Standard:** ASTM D638
- **Equipment:** Universal Testing Machine (UTM)
- **Specimens:** Dog-bone shaped or rectangular, as per standard

- **Data Collected:** Stress-strain curves, ultimate tensile strength, and modulus of elasticity
- **Instrumentation:** Digital extensometer or bonded strain gauges

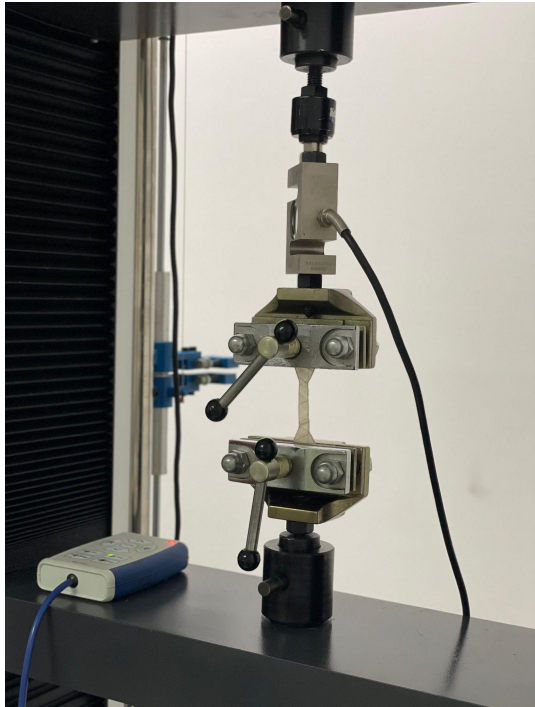


**Figure 3.13:** Tensile testing of composite laminate specimen using a Universal Testing Machine (UTM) following ASTM D638.

### 3.5.2 Bending (Flexural) Testing [28]

- **Standard:** ASTM D790
- **Test Type:** Three-point bending

- **Support span:** Typically 16 times the specimen thickness
- **Data Collected:** Load vs. deflection curves, flexural stress, flexural strain, and flexural modulus
- **Purpose:** Assess the influence of stacking sequence on out-of-plane (bending) behavior

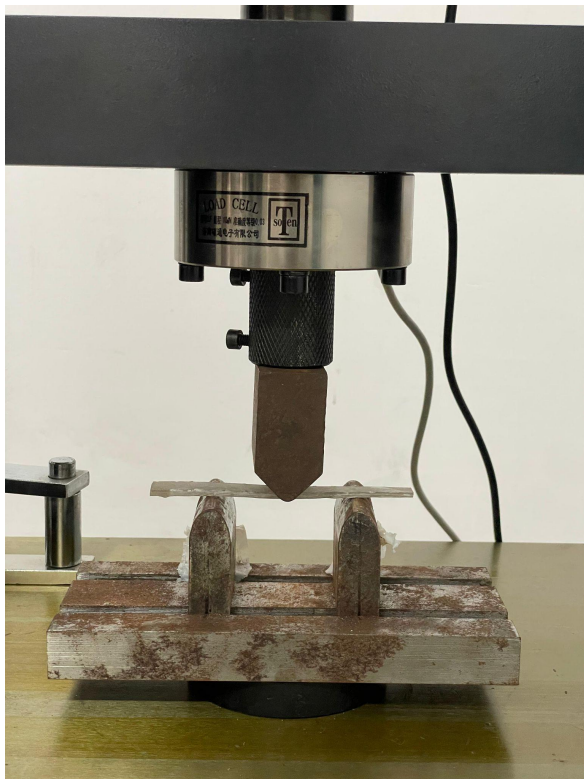


**Figure 3.15:** Three-point bending test of composite laminate specimen conducted using a Universal Testing Machine (UTM) in accordance with ASTM D790.

## 3.6 Analytical and Simulation Approach

### 3.6.1 Classical Lamination Theory (CLT)

Classical Lamination Theory (CLT) is a mathematical method used to predict the mechanical behavior of composite laminates. It calculates stress, strain, and stiffness across multiple layers based on each layer's material properties, fiber orientation, and position—without performing physical tests. Conditions include small deformations, perfect bond between layers, and negligible thickness compared to width [37].

A - Extensional stiffness matrix

B - Coupling stiffness matrix

C - Bending stiffness matrix

Q - Reduced stiffness matrix

The laminate mechanical behavior was modeled using CLT under both in-plane and bending loads:

- Calculated reduced stiffness matrix  $[Q][Q][Q]$  and its transformation  $[Q^-][\bar{Q}][Q^-]$
- Assembled global stiffness matrices  $[A][A][A]$ ,  $[B][B][B]$ , and  $[D][D][D]$  [22]
- Derived mid-plane strains, curvatures, and through-thickness distributions.
- Accounted for coupling effects due to asymmetric stacking.

### **3.6.2 MATLAB Implementation**

- Scripts developed to automate the laminate property calculation.
- Input: material constants, ply orientations, and load cases.
- Output: ply-by-ply stress, strain, and displacement fields.
- Bending loads modeled with in plane force  $N_x=1\text{kN}$  and applied moment  $M_x=10 \text{ kN.mm}$  [29].

### **3.7 Validation and Comparison**

The MATLAB analytical results were compared with experimental findings:

- Tensile test data vs. predicted stress-strain curves
- Flexural test data vs. calculated curvatures and bending stresses
- Variation in [B] and [D] matrices analyzed to interpret coupling behavior
- Differences in laminate response linked to stacking symmetry

### 3.8 A visual representation of the workflow using a structured flowchart.

The composite laminates were fabricated using the hand lay-up method with S-glass fiber (200 and 600 GSM) and unsaturated polyester resin, maintaining a 60% fiber volume fraction. Two stacking sequences were used: anti-symmetric [+60/0/-60] and asymmetric [0/±60]. The laminates were cured at room temperature for 24 hours. Specimens were cut according to ASTM D638 for tensile testing and ASTM D790 for bending tests. Mechanical tests were carried out using a Universal Testing Machine (UTM). Additionally, Classical Lamination Theory (CLT) was applied using MATLAB to calculate stress, strain, and stiffness distributions, which were compared with experimental results.

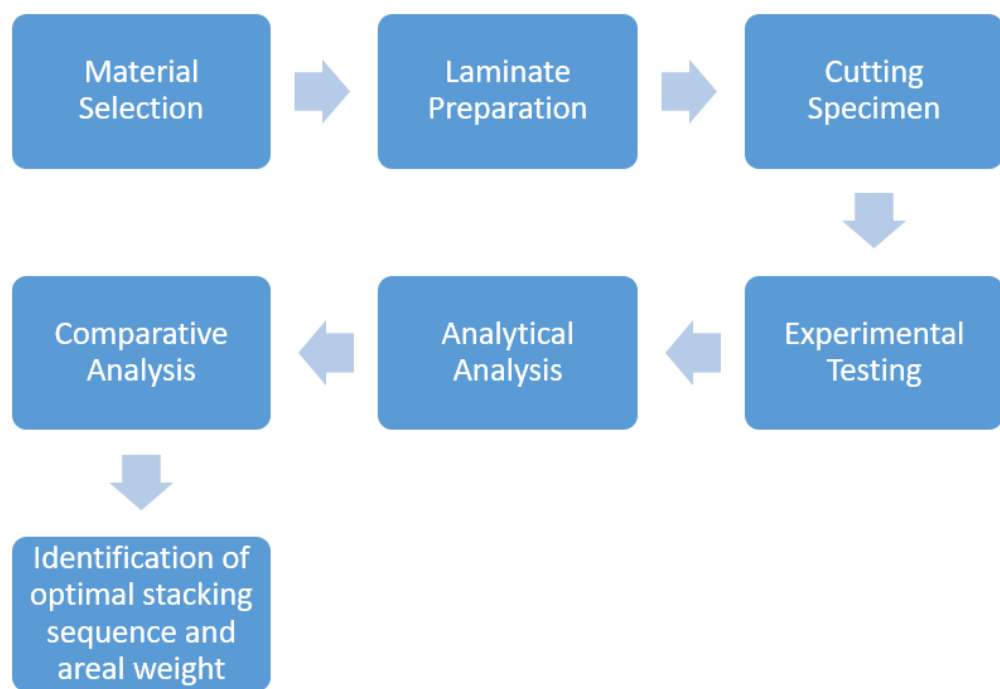


**Figure 3.16 :** A detailed flowchart representing the step-by-step workflow process.

# Chapter 4

## RESULTS AND DISCUSSION

---

### 4.1: Experimental Analysis

#### 4.1.1: Bending Test

Bending Test Stacking Sequence: [0 60 -60] GSM:200

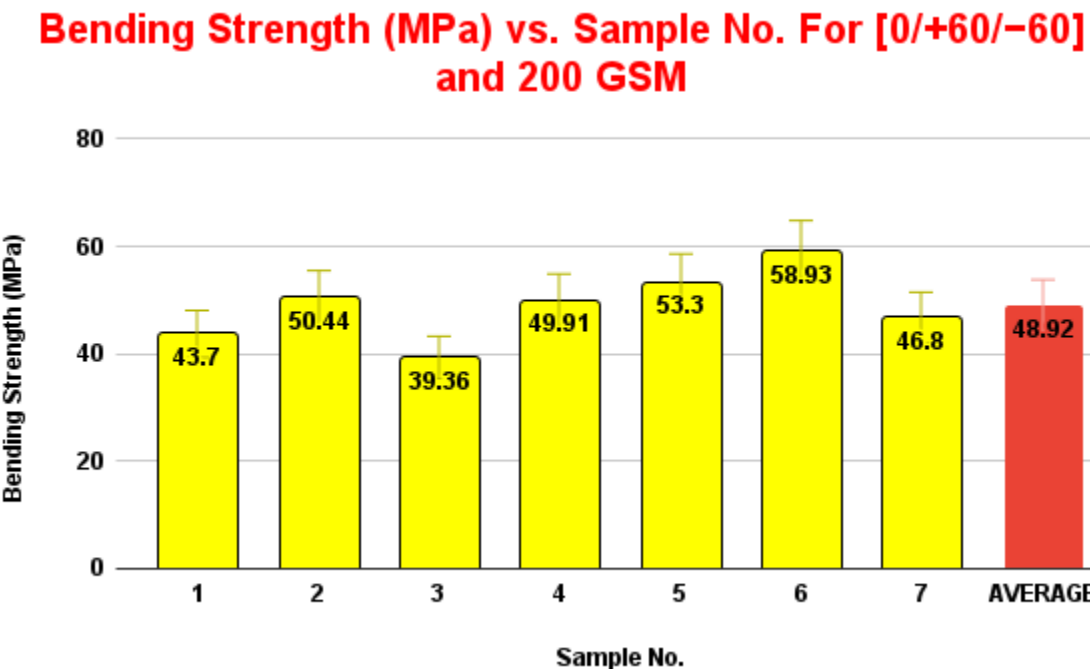


**Figure 4.1.1:** Bending strength (MPa) of asymmetric quasi-isotropic laminate with stacking sequence  $[0^\circ/+60^\circ/-60^\circ]$  using 200 gsm S-glass fiber. The graph represents individual sample results and the calculated average strength.

### **Flexural Modulus (MPa) vs. Sample No. For [0/+60/-60] and 200 GSM**

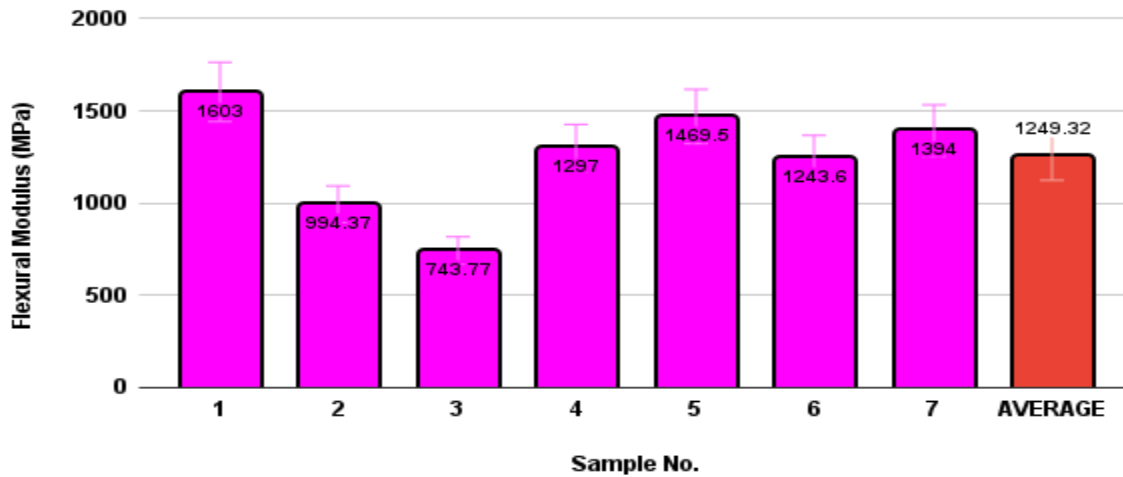


**Figure 4.1.2:** Flexural modulus (MPa) vs. Sample No. for asymmetric stacking sequence  $[0^\circ/+60^\circ/-60^\circ]$  using 200 gsm S-glass fiber composite under bending test.

### **Bending Strength (MPa) vs. Sample No. For [60/0/-60] and 200 GSM**

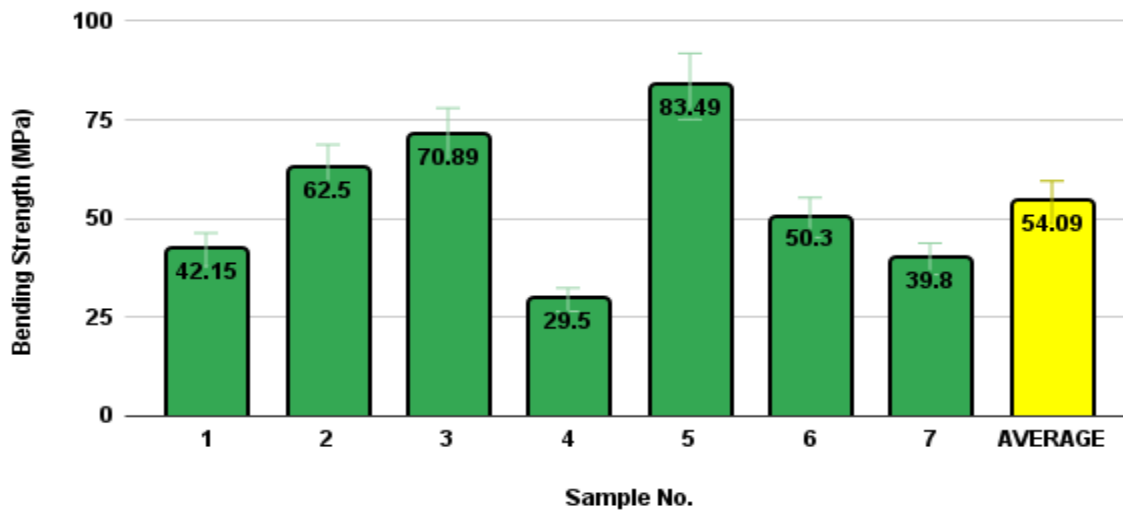


**Figure 4.1.3:** Bending strength (MPa) vs. Sample No. for anti-symmetric stacking sequence  $[+60/0/-60]$  using 200 gsm S-glass fiber composite.

### Flexural Modulus vs. Sample No. For [60/0/-60] and 200 GSM

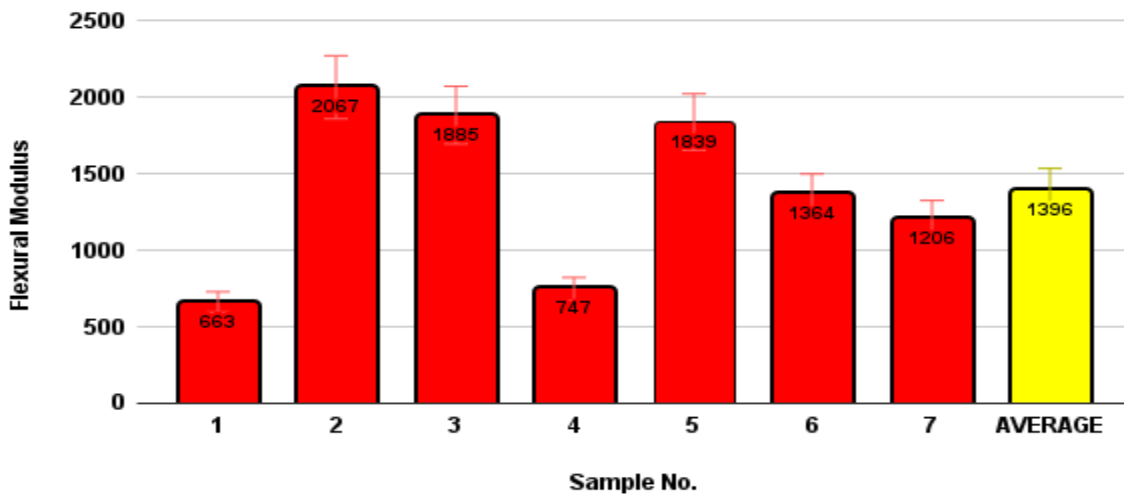


**Figure 4.1.4:** Flexural modulus (MPa) vs. Sample No. for anti-symmetric stacking sequence  $[+60/0/-60]$  using 200 gsm S-glass fiber composite.

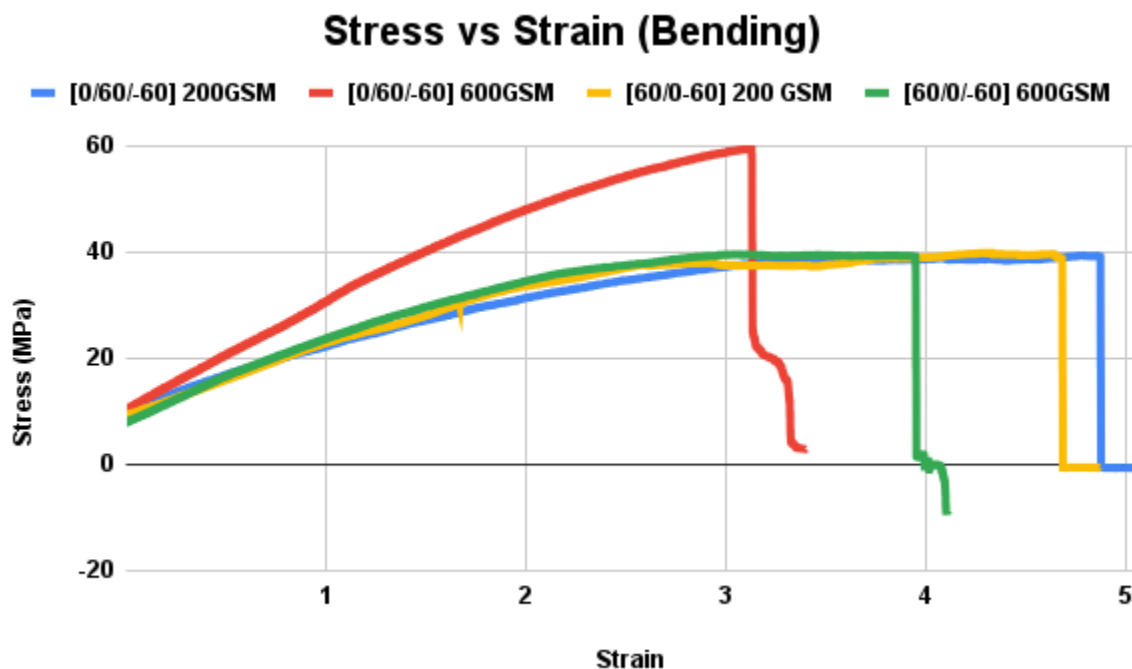


**Figure 4.1.5:** Stress - Strain curves of bending properties.

- Comparison of Bending Strength and Flexural Strength for both sequences of 200 GSM

**Bending Strength (MPa) vs. Stacking Sequence for 200 GSM**

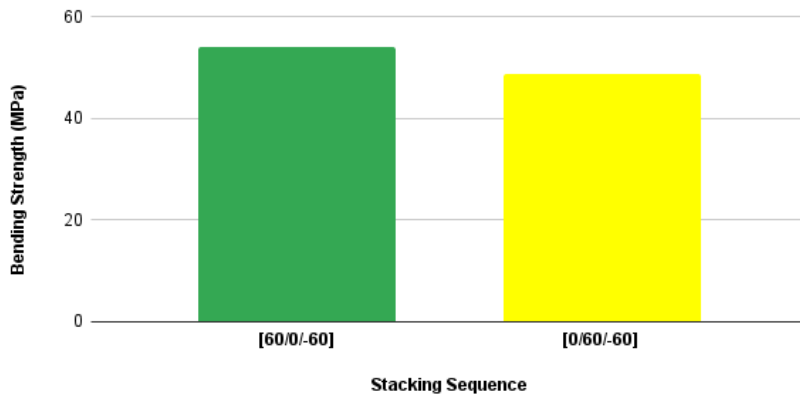


**Figure 4.1.6:** Comparison of bending strength (MPa) between anti-symmetric  $[+60^\circ/0^\circ/-60^\circ]$  and asymmetric  $[0^\circ/+60^\circ/-60^\circ]$  stacking sequences using 200 gsm.

**Flexural Strength (MPa) vs. Stacking Sequence For 200 GSM**

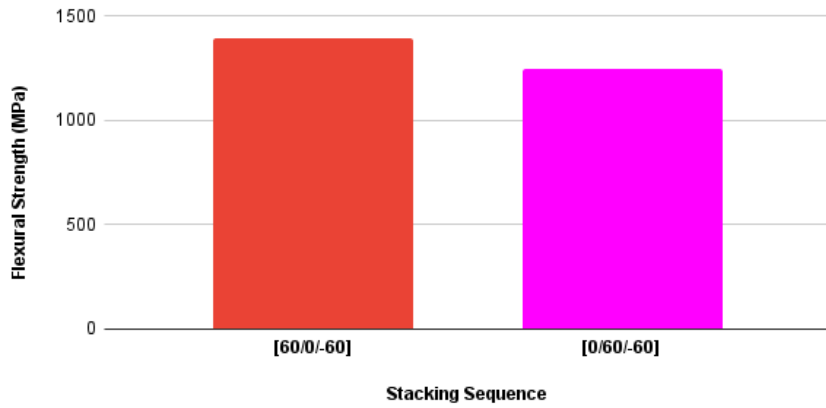


**Figure 4.1.7:** Comparison of flexural modulus (MPa) between anti-symmetric  $[+60^\circ/0^\circ/-60^\circ]$  and asymmetric  $[0^\circ/+60^\circ/-60^\circ]$  stacking sequences using 200 gsm.

**Discussion:** The results obtained from the bending tests show that the [+60/0/-60] stacking sequence achieved a higher bending strength of 54.09 MPa, compared to 48.92 MPa for the [0/+60/-60] configuration. Similarly, in the flexural test, the [+60/0/-60] laminate exhibited a superior flexural strength of 1396.07 MPa, whereas the 0/60/-60 laminate recorded a slightly lower value of 1249.32 MPa. These results clearly indicate that the [+60/0/-60] stacking sequence outperforms the [0/+60/-60] configuration in both bending and flexural strength at this specific areal weight. The enhanced mechanical properties observed in the [+60/0/-60] laminate can be attributed to its more balanced and symmetric fiber orientation, which results in improved stress distribution under mechanical loading.[30] Based on the experimental data and the mechanical behavior observed, it can be concluded that the [+60/0/-60] stacking sequence is more effective in enhancing the bending and flexural strength of S-Glass/Polyester composites at 200 GSM. This sequence is therefore considered the optimal configuration among the two for applications requiring improved flexural performance. [31]

#### 4.1.2: Tensile Test

Stacking Sequence: [60 0 -60] GSM:200

**Tensile Strength (MPa) vs. Sample No. for [60/0/-60] and 200 GSM**

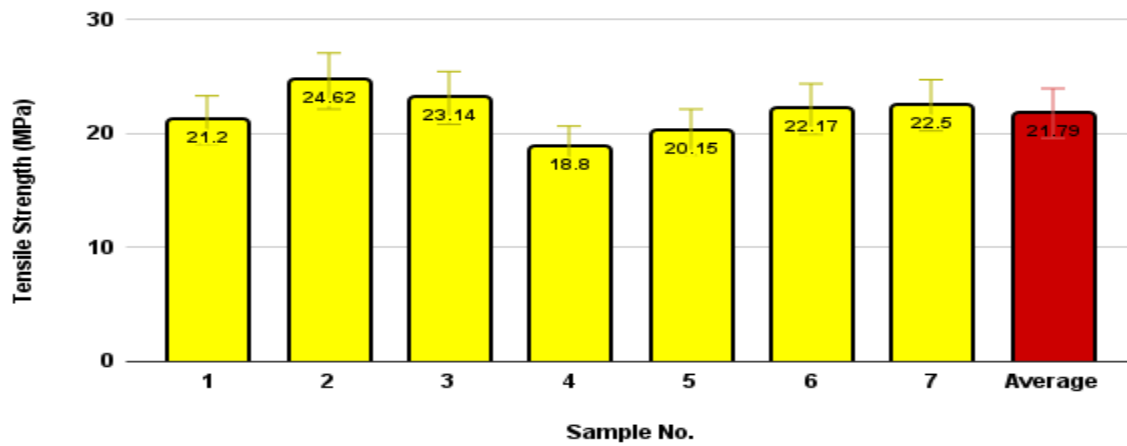


**Figure 4.1.8:** Tensile strength (MPa) vs. Sample No. for anti-symmetric stacking sequence  $[+60^\circ/0^\circ/-60^\circ]$  using 200 gsm S-glass fiber composite under tensile test.

**Tensile Modulus (MPa) vs. Sample No. for [60/0/-60] and 200 GSM**

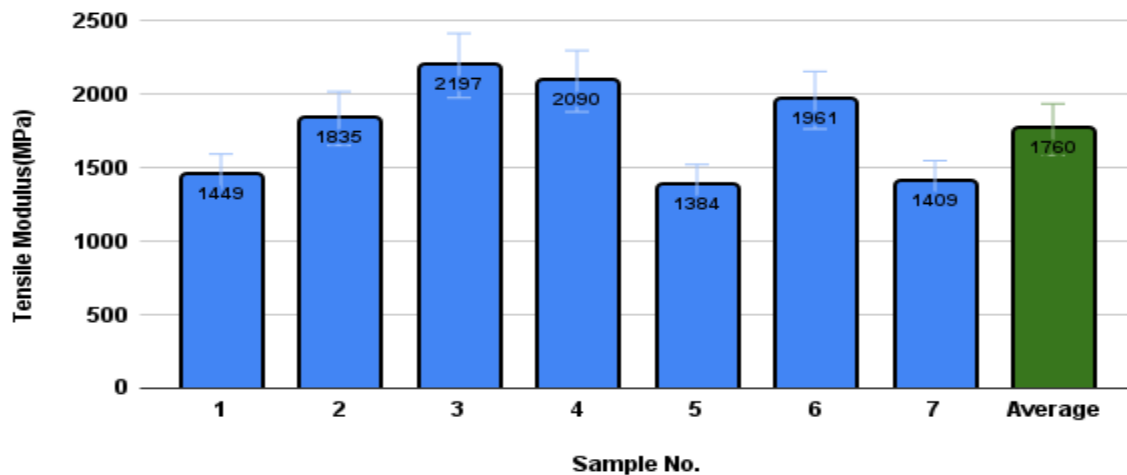


**Figure 4.1.9:** Tensile modulus (MPa) vs. Sample No. for anti-symmetric stacking sequence  $[+60^\circ/0^\circ/-60^\circ]$  using 200 gsm S-glass fiber composite under tensile test.

Tensile test: Stacking Sequence: [0 60 -60] GSM:200

### **Tensile Strength (MPa) vs. Sample No. For [0/60/-60] AND 200 GSM**

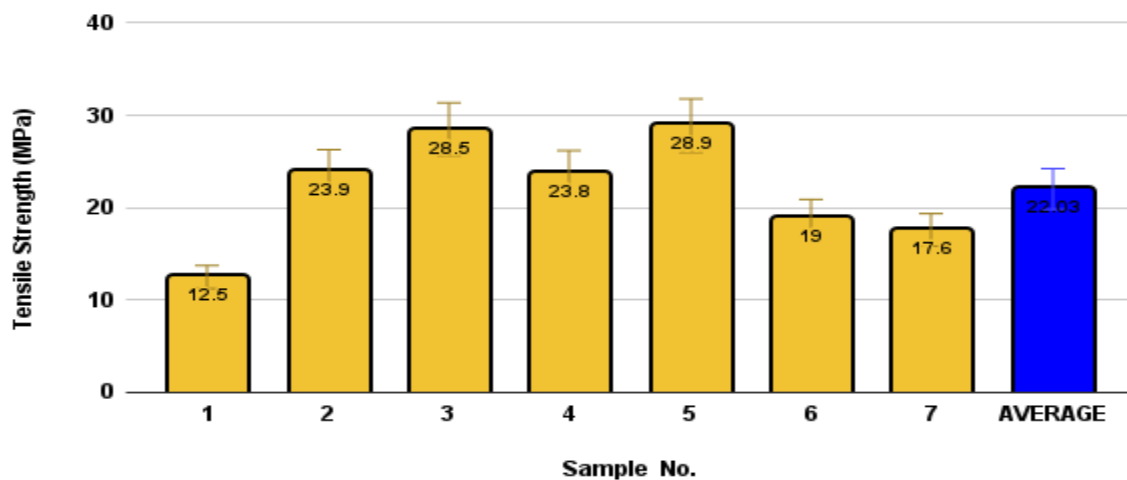


**Figure 4.1.10:** Tensile strength (MPa) vs. Sample No. for asymmetric stacking sequence  $[0^\circ/+60^\circ/-60^\circ]$  using 200 gsm S-glass fiber composite under tensile test.

### **Tensile Modulus (MPa) vs. Sample No. For [0/60/-60] AND 200 GSM**

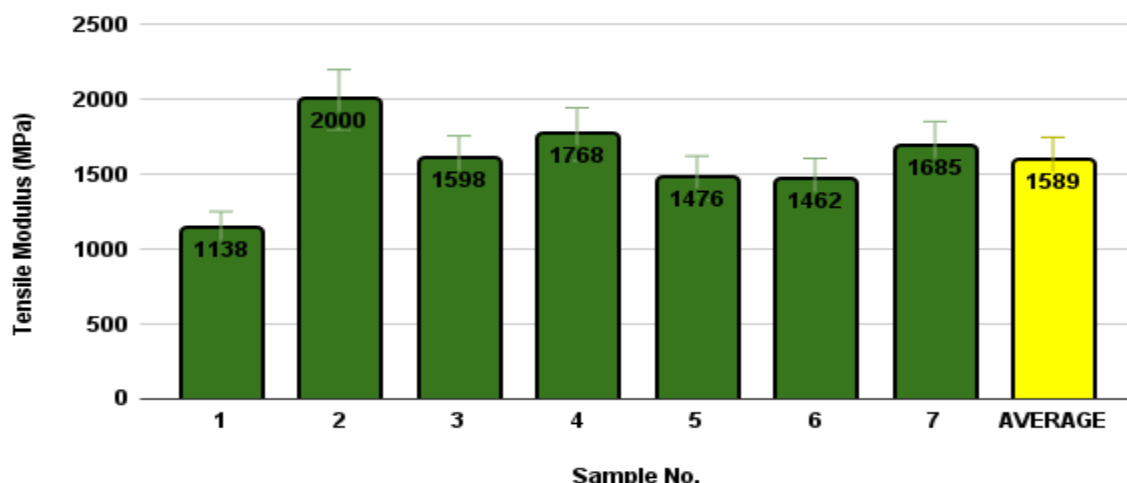


**Figure 4.1.11:** Tensile strength (MPa) vs. Sample No. for asymmetric stacking sequence  $[0^\circ/+60^\circ/-60^\circ]$  using 200 gsm S-glass fiber composite under tensile test.

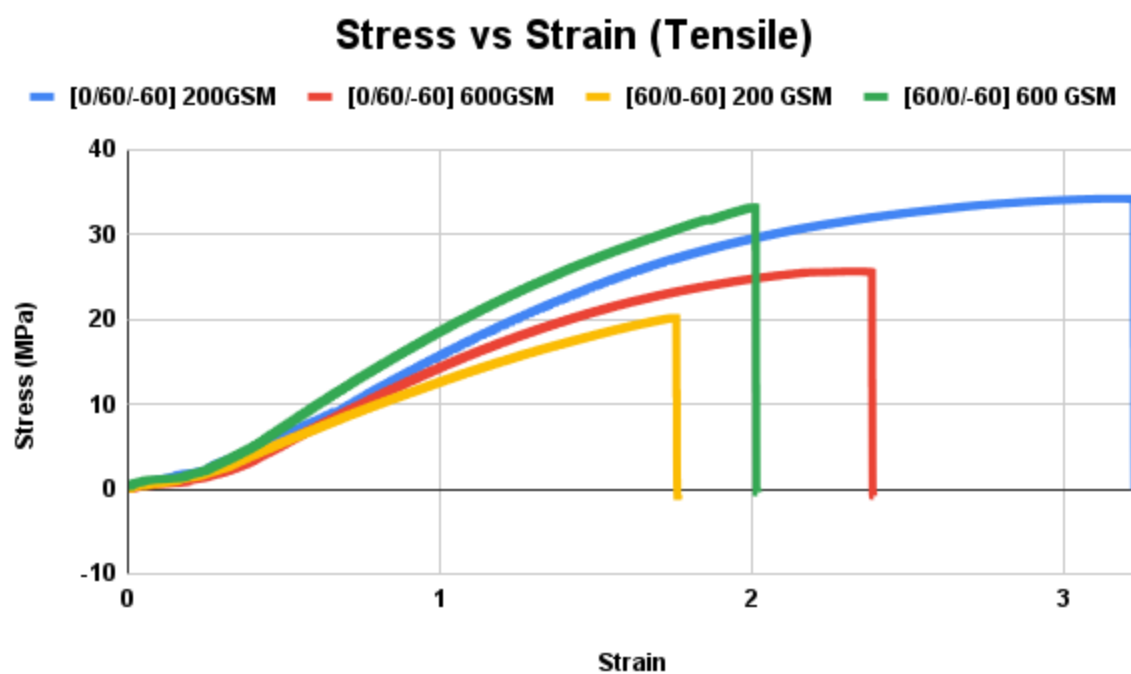


**Figure 4.1.12:** Stress - Strain curves of tensile properties.

- Comparison of Tensile Strength and Tensile Modulus for both sequences of 200 GSM

**Tensile Strength (MPa) vs. Stacking Sequence For 200 GSM**

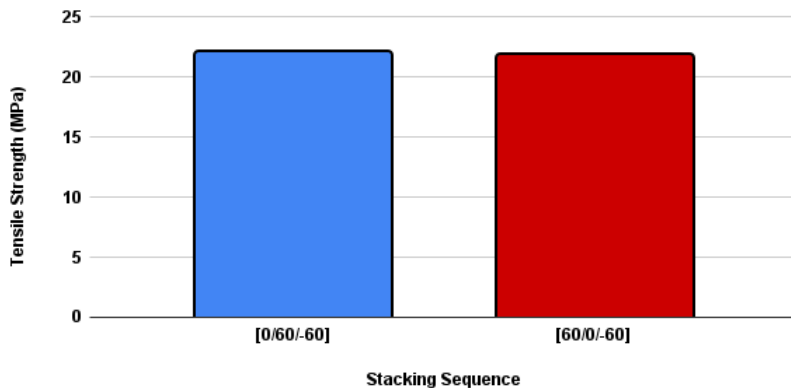


**Figure 4.1.13:** Comparison of tensile strength (MPa) between anti-symmetric  $[+60^\circ/0^\circ/-60^\circ]$  and asymmetric  $[0^\circ/+60^\circ/-60^\circ]$  stacking sequences using 200 gsm S-glass fiber composites.

**Tensile Modulus (MPa) vs. Stacking Sequence For 200 GSM**

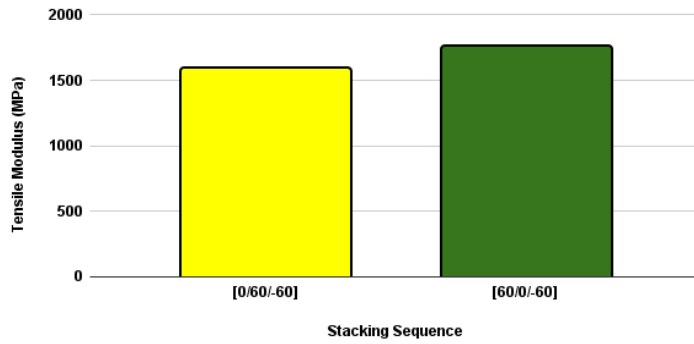


**Figure 4.1.14:** Comparison of Tensile Modulus (MPa) between anti-symmetric  $[+60^\circ/0^\circ/-60^\circ]$  and asymmetric  $[0^\circ/+60^\circ/-60^\circ]$  stacking sequences using 200 gsm S-glass fiber composites.

**Discussion:** The tensile test results reveal that the asymmetric stacking sequence [0/+60/-60] exhibits a slightly higher tensile strength of 22.03 MPa, compared to 21.8 MPa for the anti-symmetric sequence [+60/0/-60]. This marginal difference suggests that the asymmetric arrangement may offer slightly improved resistance to axial failure, possibly due to the placement of the  $\pm 60^\circ$  plies closer to the laminate surface, which could help distribute tensile stress more evenly. However, when comparing tensile modulus, the anti-symmetric laminate demonstrates a significantly higher stiffness of 1760.85 MPa, versus 1589.57 MPa for the asymmetric one. This indicates that the anti-symmetric stacking offers better resistance to elastic deformation under tensile load, likely due to its more balanced ply orientation around the mid-plane, resulting in reduced internal shear and better load transfer between layers.[30]

Based on the results, the anti-symmetric stacking sequence [+60/0/-60] is generally better for applications requiring higher stiffness and resistance to elastic deformation, as it has a significantly higher tensile modulus (1760.85 MPa).[32] On the other hand, the asymmetric sequence [0/+60/-60] offers a slightly higher tensile strength (22.03 MPa), indicating marginally better resistance to ultimate failure.

#### 4.1.3: Test Result for 600 GSM

- Comparison of Bending Strength and Flexural Modulus for both sequences of 600 GSM

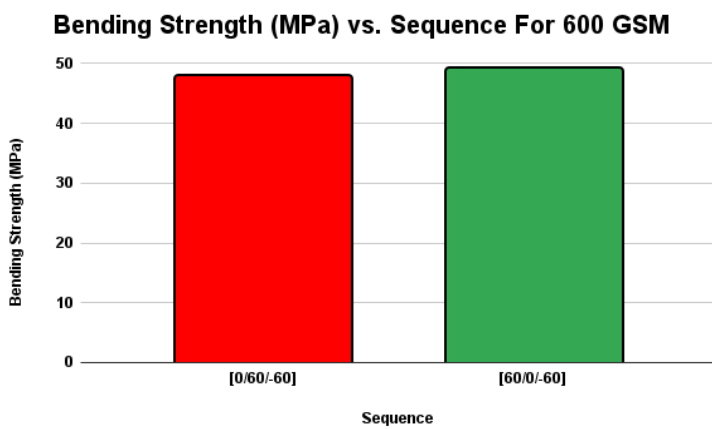


**Figure 4.1.15 :** Comparison of bending strength (MPa) between anti-symmetric [+60/0/-60] and asymmetric [0/+60/-60] stacking sequences using 600 gsm.

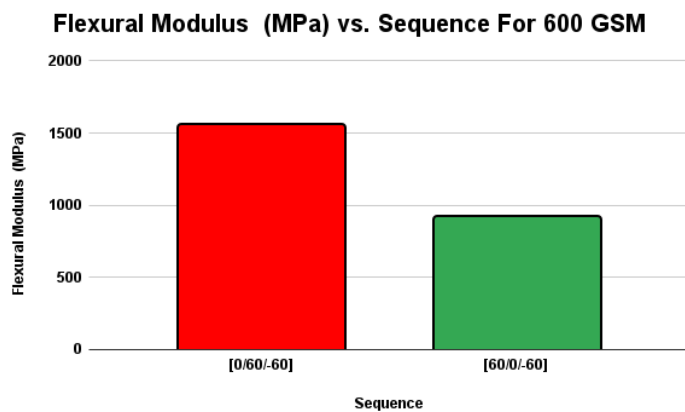


**Figure 4.1.16 :** Comparison of flexural modulus (MPa) between anti-symmetric [+60/0/-60] and asymmetric [0/+60/-60] stacking sequences using 600 gsm.

**Discussion:** From the results, the 60/0/-60 configuration exhibited a slightly higher bending strength of 49.16 MPa, compared to 47.89 MPa for the 0/60/-60 stacking. This suggests that the 60/0/-60 sequence continues to maintain its advantage in terms of bending strength, although the difference is less pronounced than at 200 GSM. However, a contrasting trend is observed in the flexural modulus, where the 0/60/-60 stacking sequence outperformed 60/0/-60. Specifically, the 0/60/-60 laminate achieved a flexural modulus of 1553.55 MPa, which is significantly higher than the 918.62 MPa recorded for the 60/0/-60 configuration. This indicates that the 0/60/-60 lay-up results in a stiffer composite under flexural loading conditions at this higher GSM.[30]

At 600 GSM, the 0/60/-60 stacking sequence is considered the optimal configuration, offering a better balance of mechanical performance, particularly due to its superior flexural stiffness, which is critical in most composite structural applications.

- Comparison of Tensile Strength and Tensile Modulus for both sequences of 600 GSM

**Tensile Strength (MPa) vs. Stacking Sequence For 600 GSM**

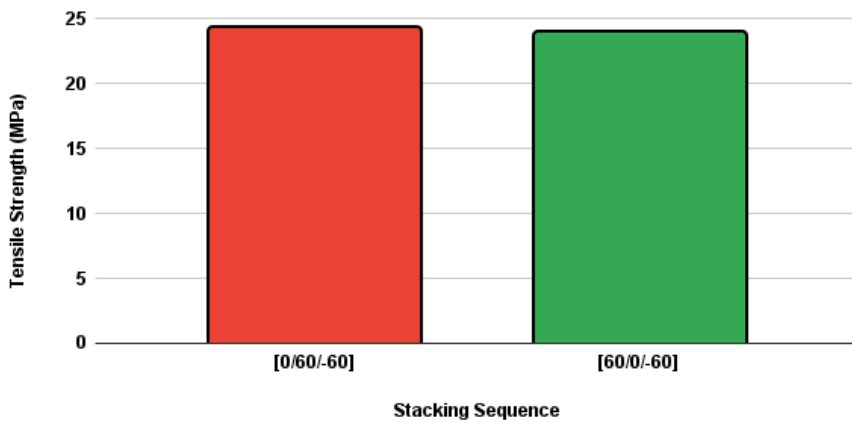


**Figure 4.1.17 :** Comparison of tensile strength (MPa) between anti-symmetric [+60/0/-60] and asymmetric [0/+60/-60] stacking sequences using 600 gsm.

**Tensile Modulus (MPa) vs. Stacking Sequence for 600 GSM**

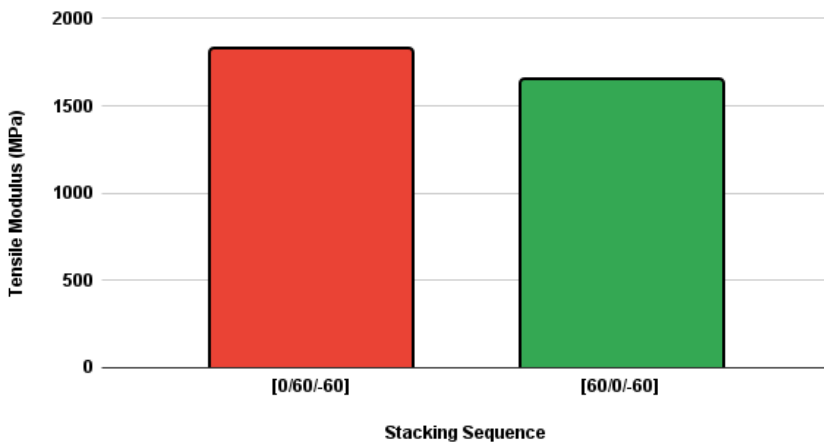


**Figure 4.1.18 :** Comparison of Tensile Modulus (MPa) between anti-symmetric [+60/0/-60] and asymmetric [0/+60/-60] stacking sequences using 600 gsm.

**Discussion:** For the 600 GSM S-Glass/Polyester composites, the 0/60/-60 stacking sequence demonstrates superior mechanical performance in both flexural and tensile behavior. It achieves a significantly higher flexural modulus of 1553.55 MPa compared to 918.62 MPa for the 60/0/-60 configuration, indicating greater stiffness under flexural loading. Additionally, in tensile testing, the 0/60/-60 sequence shows improved performance with a tensile strength of 24.33 MPa and a tensile modulus of 1822.86 MPa, both higher than those of the 60/0/-60 lay-up (23.95 MPa and 1646.50 MPa, respectively).[32] Therefore, the 0/60/-60 stacking sequence is identified as the optimal configuration for maximizing flexural and tensile properties in 600 GSM laminates.

#### 4.1.4: Test Results for Anti-Symmetric Stacking Sequence [+60/0/-60]

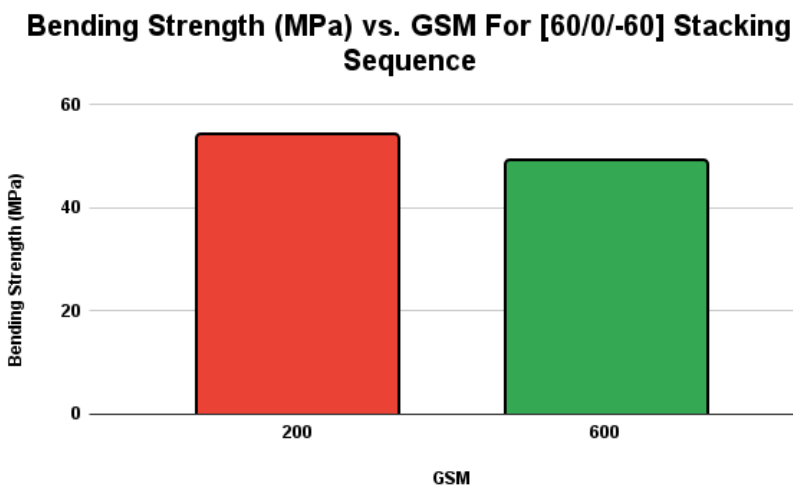


**Figure 4.1.19 :** Comparison of Bending Strength for the Same Stacking Sequence [+60/0/-60] at 200 GSM and 600 GSM.

**Flexural Modulus (MPa) vs. GSM For [60/0/-60] Stacking Sequence**

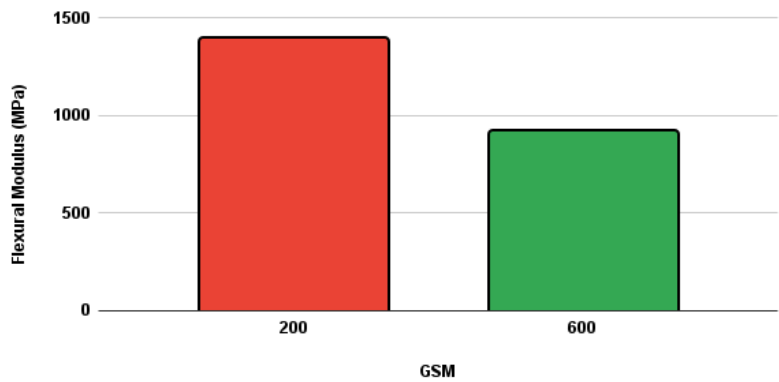


**Figure 4.1.20 :** Comparison of Flexural Modulus for the Same Stacking Sequence [+60/0/-60] at 200 GSM and 600 GSM.

**Tensile Strength (MPa) vs. GSM For [60/0/-60] Stacking Sequence**

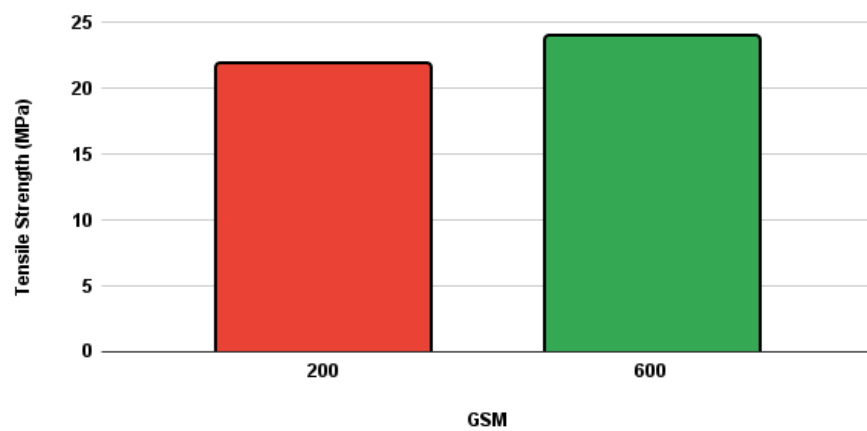


**Figure 4.1.21 :** Comparison of Tensile Strength for the Same Stacking Sequence [+60/0/-60] at 200 GSM and 600 GSM.

### Tensile Modulus (MPa) vs. GSM For [60/0/-60] Stacking Sequence

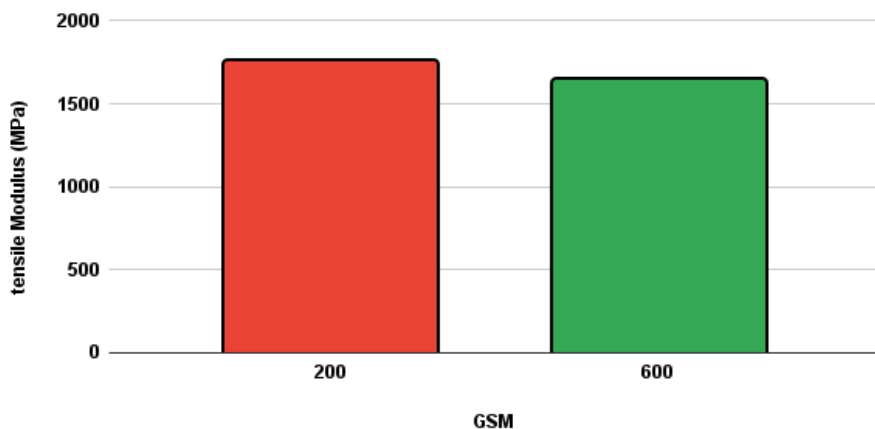


**Figure 4.1.22 :** Comparison of Tensile Modulus for the Same Stacking Sequence [+60/0/-60] at 200 GSM and 600 GSM.

**Discussion:** Effect of GSM on Mechanical Properties for Fixed Stacking Sequence [+60/0/-60].

In bending tests, the 200 gsm laminate exhibits superior performance with a bending strength of 54.09 MPa and a flexural modulus of 1396.07 MPa, compared to 49.16 MPa and 918.62 MPa, respectively, for the 600 gsm laminate. This suggests that thinner laminates (with lower GSM) provide better flexural rigidity and surface bonding quality, likely due to better resin impregnation and fewer internal voids.

However, in tensile tests, the 600 gsm laminate shows improved tensile strength (23.95 MPa) over the 200 gsm laminate (21.8 MPa), indicating higher load-bearing capacity in the fiber direction due to greater fiber content. Despite this, the tensile modulus remains slightly higher in the 200 gsm sample (1760.85 MPa vs. 1646.5 MPa), meaning the lower GSM laminate is still stiffer under tension.

In summary:

- **200 gsm** offers better bending performance and overall stiffness
- **600 gsm** offers better tensile strength

The selection depends on the application:

- Use **200 gsm** if stiffness and flexural performance are critical.
- Use **600 gsm** where tensile load-bearing capacity is prioritized.

#### 4.1.5: Test Results for Asymmetric Stacking Sequence [0/+60/-60]

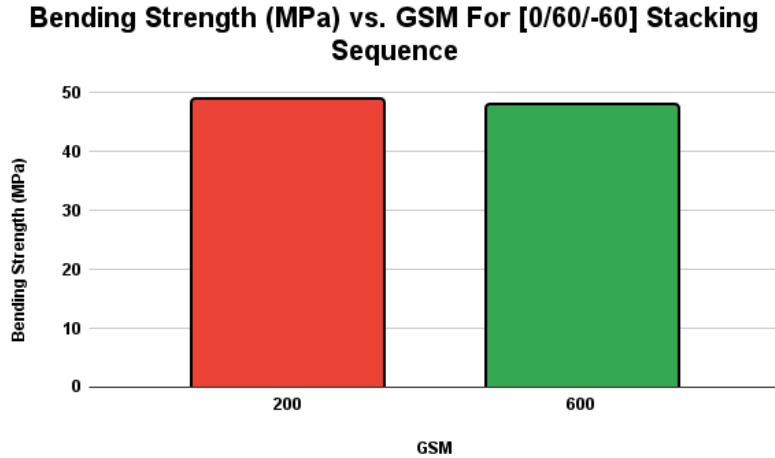


**Figure 4.1.23 :** Comparison of Bending Strength for the Same Stacking Sequence [0/+60/-60] at 200 GSM and 600 GSM.

### **Flexural Modulus (MPa) vs. GSM For [0/60/-60] Stacking Sequence**

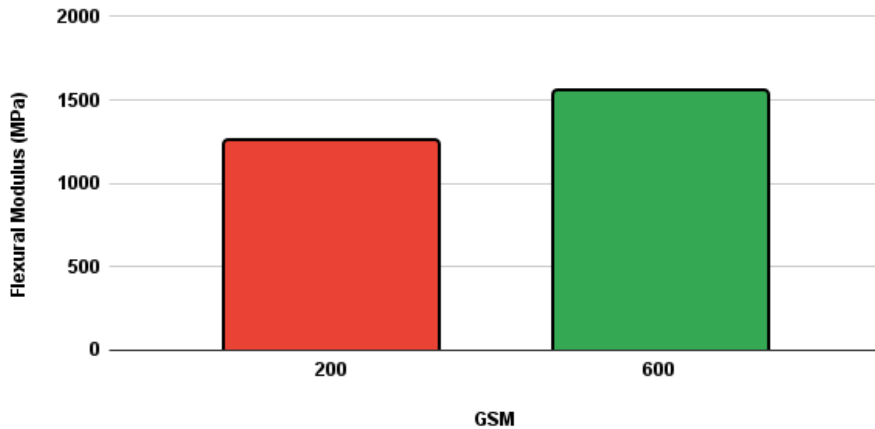


**Figure 4.1.24 :** Comparison of Flexural Modulus for the Same Stacking Sequence [0/+60/-60] at 200 GSM and 600 GSM.

### **Tensile Strength (MPa) vs. GSM For [0/60/-60] Stacking Sequence**

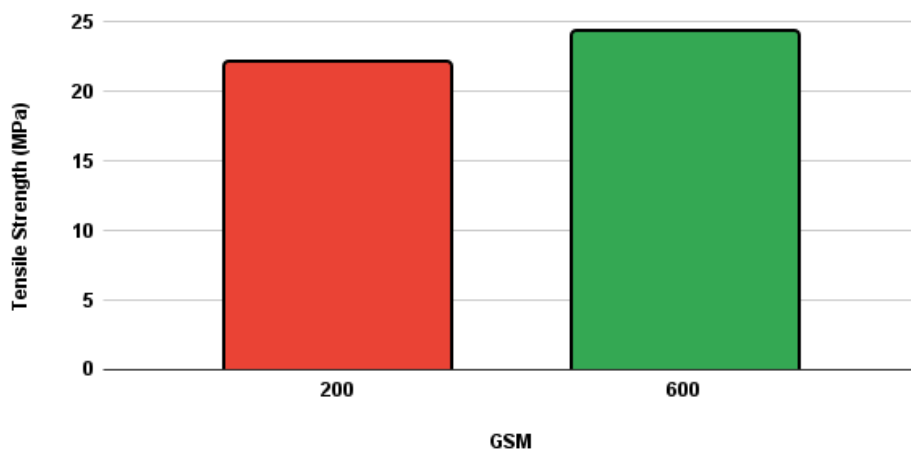


**Figure 4.1.25 :** Comparison of Tensile Strength for the Same Stacking Sequence [0/+60/-60] at 200 GSM and 600 GSM

### Tensile Modulus (MPa) vs. GSM For [0/60/-60] Stacking Sequence

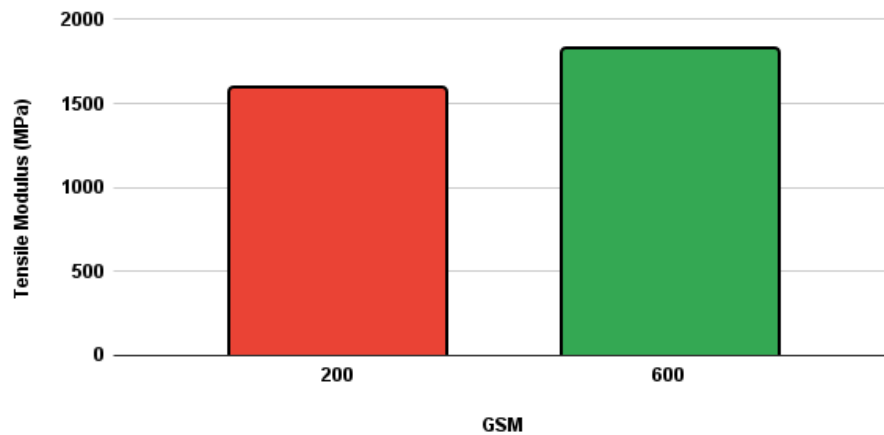


**Figure 4.1.26 :** Comparison of Tensile Modulus for the Same Stacking Sequence [0/+60/-60] at 200 GSM and 600 GSM

**Discussion:** Effect of GSM on Mechanical Properties for Fixed Stacking Sequence [0/+60/-60].

In the bending test, both GSMS show similar bending strength, with 200 gsm slightly higher at 48.92 MPa, compared to 47.89 MPa for 600 gsm. However, 600 gsm exhibits a significantly higher flexural modulus (1553.55 MPa) than 200 gsm (1249.32 MPa), indicating better stiffness and resistance to bending deformation, likely due to its increased thickness and fiber volume.

In the tensile test, 600 gsm outperforms 200 gsm in both tensile strength (24.33 MPa vs. 22.03 MPa) and tensile modulus (1822.86 MPa vs. 1589.57 MPa). The increased fiber mass in 600 gsm laminates provides improved load-carrying capacity and stiffness under axial loading, making it more suitable for tension-dominant applications.

- **200 gsm:** Slightly better bending strength

- **600 gsm:** Better in flexural modulus, tensile strength, and tensile modulus

Therefore, for this stacking sequence, 600 gsm shows superior overall mechanical performance, especially in stiffness and tensile properties, while 200 gsm may offer slight advantages in bending strength where lightweight or thinner profiles are desired.

## 4.2: Analytical Analysis

### 4.2.1: Classic Laminate Theory Code

This section of the report details the code used to estimate the influence of the stacking sequence on stress and strain distributions in MATLAB. The code takes user input for various parameters and calculates A, B and D matrices. As well as provide the stress and strain distribution over all the layers. Calculations were performed using MATLAB software for computational efficiency

#### Code for A, B and D matrices:

```
%% 1. Material properties
Ef = 85.5; Em = 4.0; % GPa
Gf = 26.72; Gm = 1.44; % GPa
vf = 0.22; vm = 0.39;
Vf = 0.6; Vm = 1-Vf;

E1 = Ef*Vf + Em*Vm;
E2 = (Ef*Em)/(Ef*Vm + Em*Vf);
G12 = (Gf*Gm)/(Gf*Vm + Gm*Vf);
nu12 = vf*Vf + vm*Vm;
```

```

nu21 = nu12*E2/E1;

Q11 = E1/(1-nu12*nu21);
Q22 = E2/(1-nu12*nu21);
Q12 = nu12*E2/(1-nu12*nu21);
Q66 = G12;
Qred = [Q11 Q12 0; Q12 Q22 0; 0 0 Q66]; % kN/mm2

%% 2. Two stacking sequences

plyThk = 0.4; % mm
stacks(1).name = '[+60/0/-60] anti-sym';
stacks(1).angles = [ 60 0 -60];
stacks(2).name = '[0/+60/-60] asym';
stacks(2).angles = [ 0 60 -60];

for s = 1:2
    ang = stacks(s).angles;
    n = numel(ang);
    z = linspace(-n*plyThk/2, n*plyThk/2, n+1); % ply interfaces

    [A,B,D] = buildABD(Qred, ang, z);
    stacks(s).A = A; stacks(s).B = B; stacks(s).D = D;

    fprintf('\n==== %s ====\n', stacks(s).name);
    fprintf('[A] (kN/mm)\n'); disp(A);
    fprintf('[B] (kN)\n'); disp(B);
    fprintf('[D] (kN·mm)\n'); disp(D);

```

```

end

function [A,B,D] = buildABD(Qred,stack,z)

A = zeros(3); B = zeros(3); D = zeros(3);

for k = 1:numel(stack)

Qb = QbarCS(Qred, stack(k));

zk = z(k+1); zk1 = z(k);

A = A + Qb*(zk - zk1);

B = B + 0.5*Qb*(zk^2 - zk1^2);

D = D + (1/3)*Qb*(zk^3 - zk1^3);

end

end

function Qb = QbarCS(Q,theta)

c = cosd(theta); s = sind(theta); c2=c^2; s2=s^2; c4=c2^2; s4=s2^2;

Q11=Q(1,1); Q22=Q(2,2); Q12=Q(1,2); Q66=Q(3,3);

Qb11 = Q11*c4 + 2*(Q12+2*Q66)*c2*s2 + Q22*s4;

Qb22 = Q11*s4 + 2*(Q12+2*Q66)*c2*s2 + Q22*c4;

Qb12 = (Q11+Q22-4*Q66)*c2*s2 + Q12*(c4+s4);

Qb66 = (Q11+Q22-2*Q12-2*Q66)*c2*s2 + Q66*(c4+s4);

Qb16 = (Q11-Q12-2*Q66)*c^3*s - (Q22-Q12-2*Q66)*c*s^3;

Qb26 = (Q11-Q12-2*Q66)*c*s^3 - (Q22-Q12-2*Q66)*c^3*s;

Qb = [Qb11 Qb12 Qb16; Qb12 Qb22 Qb26; Qb16 Qb26 Qb66];

end

```

#### 4.2.2:Results Provided by Code:

6/25/25 2:28 AM MATLAB Command Window 1 of 1

```

==== [+60/0/-60] anti-sym ====
[A] (kN/mm)
31.2442  9.9351      0
9.9351  31.2442      0
0        0        10.6546

[B] (kN)
0        0      -1.5250
0        0      -4.6000
-1.5250  -4.6000      0

[D] (kN·mm)
1.9797  1.5473      0
1.5473  4.8087      0
0        0        1.6336

==== [0/+60/-60] asym ====
[A] (kN/mm)
31.2442  9.9351      0.0000
9.9351  31.2442      0.0000
0.0000  0.0000  10.6546

[B] (kN)
-6.6359  1.3315     -0.7625
1.3315  3.9729     -2.3000
-0.7625  -2.3000     1.3315

[D] (kN·mm)
4.6341  1.0147     -0.3050
1.0147  3.2196     -0.9200
-0.3050  -0.9200     1.1010

~~

```

**Fig 4.2.1: MATLAB Command Window for A, B and D matrices**

#### 4.2.3: Code For Strain and Stress Distribution on Laminate Thickness:

```

%% 1. Material properties
Ef = 85.5; Em = 4.0;    % GPa
Gf = 26.72; Gm = 1.44;   % GPa
vf = 0.22; vm = 0.39;
Vf = 0.6; Vm = 1 - Vf;
E1 = Ef*Vf + Em*Vm;
E2 = (Ef*Em)/(Ef*Vm + Em*Vf);

```

```

G12 = (Gf*Gm)/(Gf*Vm + Gm*Vf);

nu12 = vf*Vf + vm*Vm;

nu21 = nu12 * E2 / E1;

Q11 = E1/(1 - nu12*nu21);

Q22 = E2/(1 - nu12*nu21);

Q12 = nu12*E2/(1 - nu12*nu21);

Q66 = G12;

Qred = [Q11 Q12 0; Q12 Q22 0; 0 0 Q66]; % kN/mm2

```

## **%% 2. Stack definitions**

```

plyThk = 0.4;

stacks(1).name = '[+60/0/-60] Anti-symmetric';

stacks(1).angles = [ 60 0 -60];

stacks(2).name = '[0/+60/-60] Asymmetric';

stacks(2).angles = [ 0 60 -60];

```

## **%% 3. Loop through both stacks**

```

for s = 1:2

ang = stacks(s).angles;

n = numel(ang);

z = linspace(-n*plyThk/2, n*plyThk/2, n+1);

```

```

[A,B,D] = buildABD(Qred, ang, z);

ABD = [A B; B D];

stacks(s).A = A; stacks(s).B = B; stacks(s).D = D;

```

```

% Apply in-plane & bending loads

N = [1; 0; 0]; % kN/mm

M = [10; 0; 0]; % kN·mm/mm

loadVec = [N; M];

x = ABD \ loadVec;

eps0 = x(1:3); kappa = x(4:6);

% Stress and strain through thickness

zEval = linspace(z(1), z(end), 200);

strainZ = zeros(3,numel(zEval));

stressZ = zeros(3,numel(zEval));

for j = 1:numel(zEval)

    zj = zEval(j);

    strain = eps0 + zj * kappa;

    ply = find(z(1:end-1) <= zj & z(2:end) >= zj, 1);

    Qbar = QbarCS(Qred, ang(ply));

    stress = Qbar * strain;

    strainZ(:,j) = strain;

    stressZ(:,j) = stress;

end

% Store for plotting

stacks(s).zEval = zEval;

stacks(s).strainZ = strainZ;

stacks(s).stressZ = stressZ;

```

```

end

%% 4. Plotting

for s = 1:2

zEval = stacks(s).zEval;
strainZ = stacks(s).strainZ;
stressZ = stacks(s).stressZ;

figure('Name', ['Strain - ' stacks(s).name]);
plot(strainZ(1,:),zEval,'r', strainZ(2,:),zEval,'g', strainZ(3,:),zEval,'b');
xlabel('Strain'); ylabel('z (mm)'); grid on;
legend('\epsilon_x','\epsilon_y','\gamma_xy');
title(['Mid-plane Strain Distribution: ' stacks(s).name]);

figure('Name', ['Stress - ' stacks(s).name]);
plot(stressZ(1,:),zEval,'r', stressZ(2,:),zEval,'g', stressZ(3,:),zEval,'b');
xlabel('Stress (kN/mm2)'); ylabel('z (mm)'); grid on;
legend('\sigma_x','\sigma_y','\tau_xy');
title(['Stress Distribution: ' stacks(s).name]);
end

%% 5. Export CSV

for s = 1:2

writematrix([stacks(s).zEval.' stacks(s).strainZ.'], ['strain_ ' sName(stacks(s).name) '.csv']);
writematrix([stacks(s).zEval.' stacks(s).stressZ.'], ['stress_ ' sName(stacks(s).name) '.csv']);

end

```

```

function Qb = QbarCS(Q,theta)
c = cosd(theta); s = sind(theta); c2=c^2; s2=s^2; c4=c2^2; s4=s2^2;
Q11=Q(1,1); Q22=Q(2,2); Q12=Q(1,2); Q66=Q(3,3);
Qb11 = Q11*c4 + 2*(Q12+2*Q66)*c2*s2 + Q22*s4;
Qb22 = Q11*s4 + 2*(Q12+2*Q66)*c2*s2 + Q22*c4;
Qb12 = (Q11+Q22-4*Q66)*c2*s2 + Q12*(c4+s4);
Qb66 = (Q11+Q22-2*Q12-2*Q66)*c2*s2 + Q66*(c4+s4);
Qb16 = (Q11-Q12-2*Q66)*c^3*s - (Q22-Q12-2*Q66)*c*s^3;
Qb26 = (Q11-Q12-2*Q66)*c*s^3 - (Q22-Q12-2*Q66)*c^3*s;
Qb = [Qb11 Qb12 Qb16; Qb12 Qb22 Qb26; Qb16 Qb26 Qb66];
end

function [A,B,D] = buildABD(Qred,angles,z)
A = zeros(3); B = zeros(3); D = zeros(3);
for k = 1:numel(angles)
    Qb = QbarCS(Qred, angles(k));
    zk = z(k+1); zk1 = z(k);
    A = A + Qb*(zk - zk1);
    B = B + 0.5*Qb*(zk^2 - zk1^2);
    D = D + (1/3)*Qb*(zk^3 - zk1^3);
end
end

function tag = sName(name)
tag = lower(regexprep(name,'[^a-zA-Z0-9]','_'));
end

```

**Result Provided by this Code:**

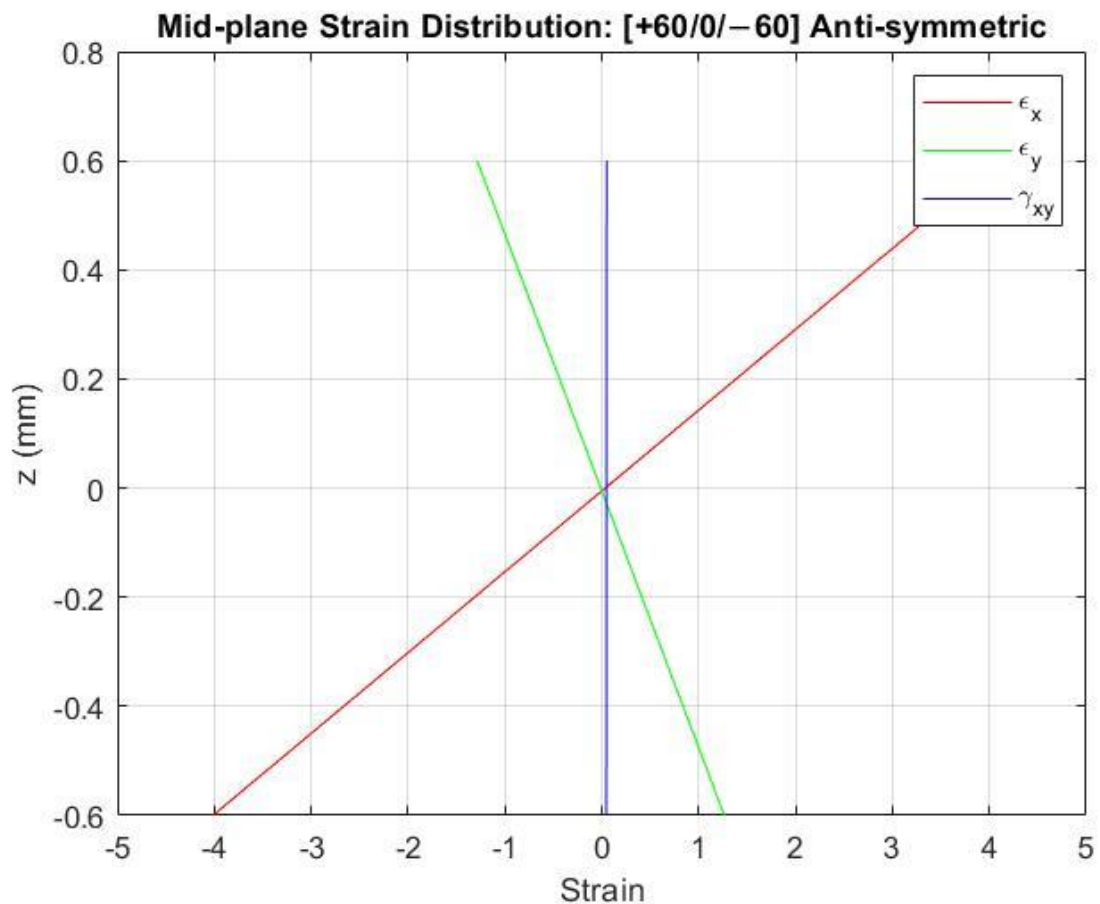


**Fig 4.2.2: Mid-plane Strain Distribution: [+60/0/-60] Anti-Symmetric**

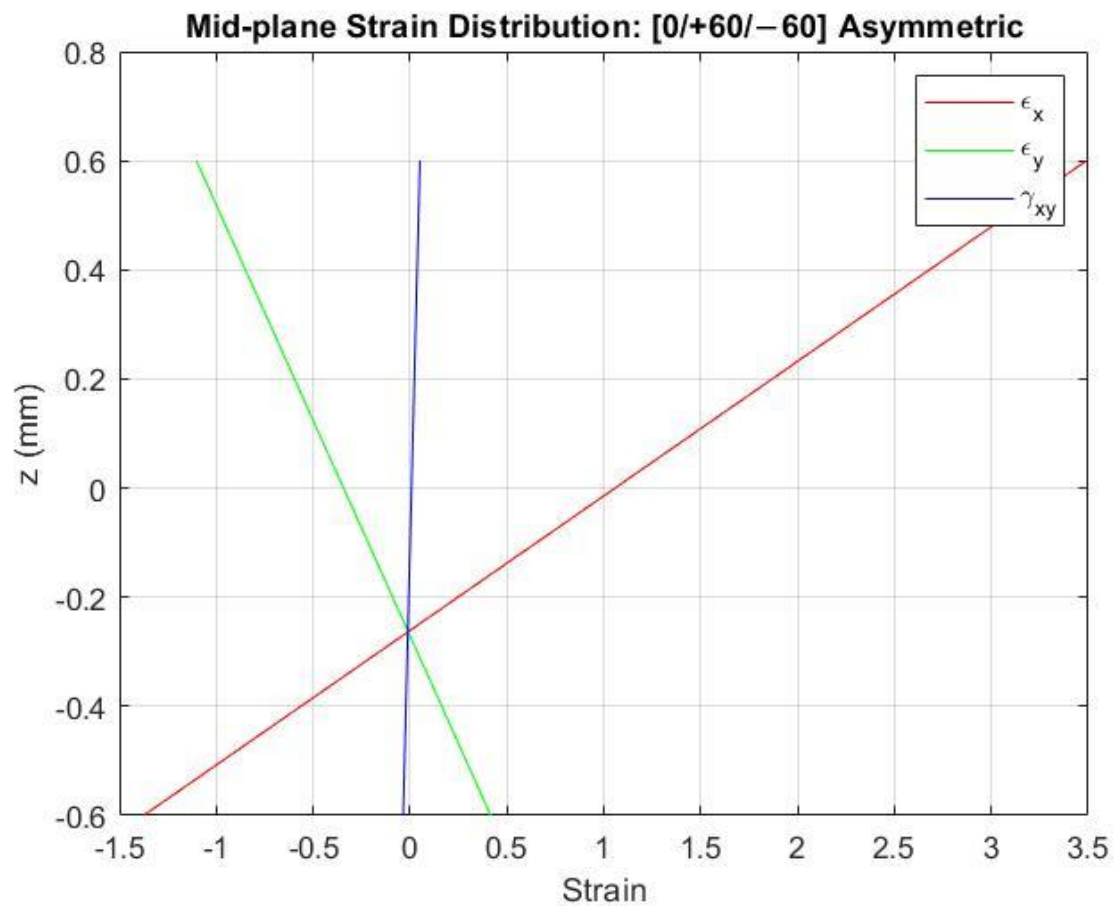


**Fig 4.2.3: Mid-plane Strain Distribution: [0/+60/-60] Asymmetric**

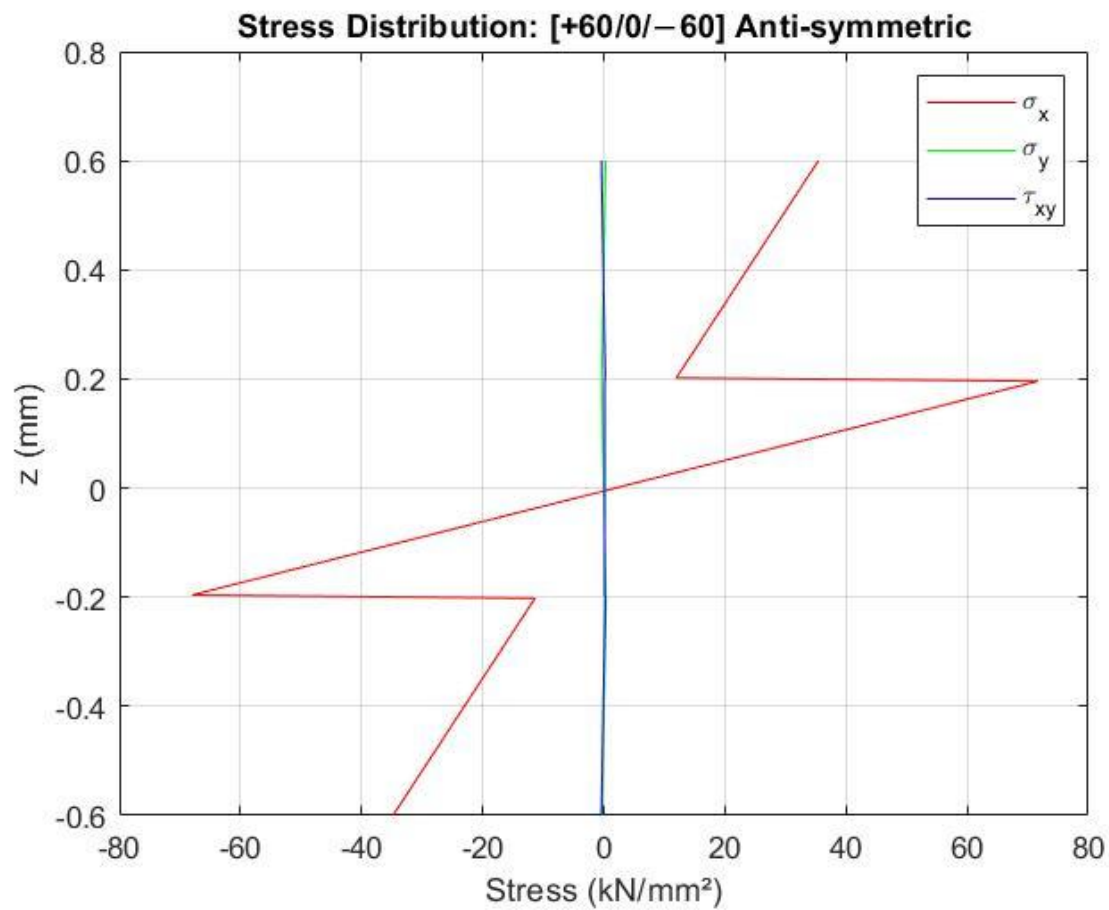


**Fig 4.2.4: Stress Distribution: [+60/0/-60] Anti-symmetric**

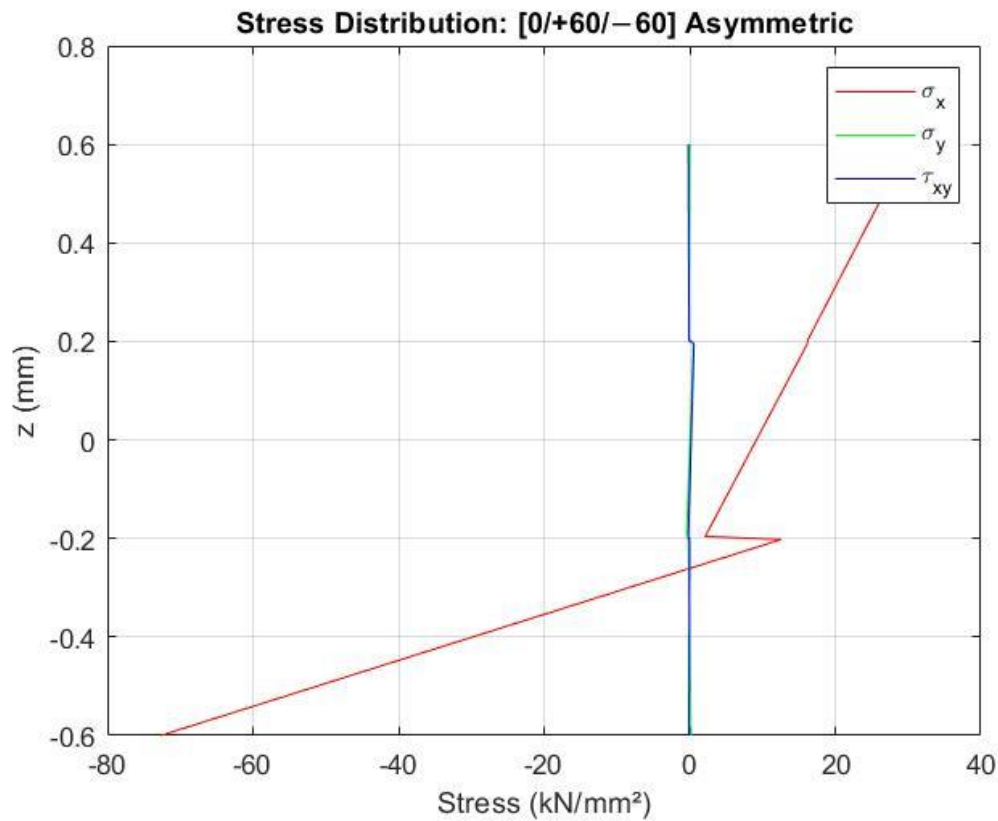


**Fig 4.2.5: Stress Distribution: [0/+60/-60] Asymmetric**

[+60/0/-60]		$\sigma_x$	$\sigma_y$	$\tau_{xy}$
$i=1$	sup.	-34.11	0.301	-0.402
	inf.	-11.36	0.375	0.253
$i=2$	sup.	-68	0.321	0.161
	$z=0$	2.1	0	0.166
	inf.	71.76	-0.34	0.169
$i=3$	sup.	11.99	-0.353	0.236
	inf.	35.44	0.301	-0.4

**Table 4.2.1: Stress Distribution Values for [+60/0/-60] Anti-symmetric**

### Tensile Stress Calculation for [+60/0/-60] Anti-symmetric Laminate:

$\sigma_{x=1}$ , for  $i=1$ ,  $(-34.11-11.36) = -45.47$  MPa

So, layer 1 faces Compressive Stress.

$\sigma_{x=2}$ , for  $i=2$ ,  $(-68+2.1+71.76) = 5.86$  MPa

So, layer 2 faces Tensile Stress.

$\sigma_{x=3}$ , for  $i=3$ ,  $(11.99+35.44) = 47.43$  MPa

So, layer 3 faces Tensile Stress.

So, Overall Tensile Stress =  $(\sigma_{x=1} + \sigma_{x=2} + \sigma_{x=3})/3 = (0 + 5.86 + 47.43)/3 = 17.76$  MPa

[0/+60/-60]		$\sigma_x$	$\sigma_y$	$T_{xy}$
$i=1$	sup.	-72.67	0.185	-0.117
	inf.	12.58	-0.175	-0.022
$i=2$	sup.	2.14	-0.44	-0.185
	$z=0$	9.27	0.045	0.208
	inf.	16.36	0.533	0.601
$i=3$	sup.	16.19	0.117	-0.075
	inf.	30.198	0.029	-0.196

Table 4.2.2: Stress Distribution for [0/+60/-60] Asymmetric

### Tensile Stress Calculation for [0/+60/-60] Asymmetric Laminate:

$\sigma_{x=1}$ , for  $i=1$ ,  $(-72.67+12.58) = -60.09$  MPa

So, layer 1 faces Compressive Stress.

$\sigma_{x=2}$ , for  $i=2$ ,  $(2.14+9.27+16.36) = 27.77$  MPa

So, layer 2 faces Tensile Stress.

$\sigma_{x=3}$ , for  $i=3$ ,  $(16.19+30.198) = 46.39$  MPa

So, layer 3 faces Tensile Stress.

So, Overall Tensile Stress =  $(\sigma_{x=1} + \sigma_{x=2} + \sigma_{x=3})/3 = (0 + 27.77 + 46.39)/3 = 24.72$  MPa

#### 4.2.4: Superimposed Graphs

The graphs of stress and strain distribution for both stacking sequences were superimposed for better understanding of the stress and strain distributions. Matplotlib software was used to superimpose these graphs.

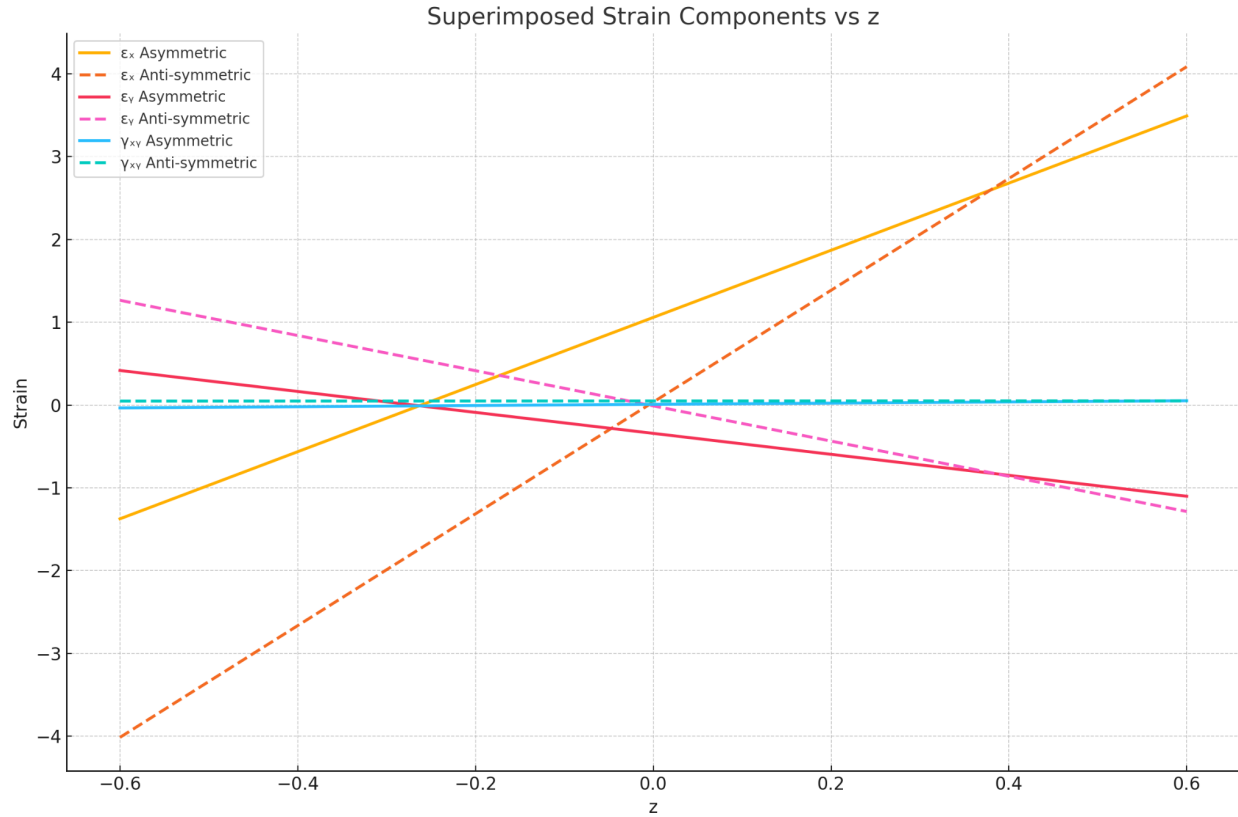
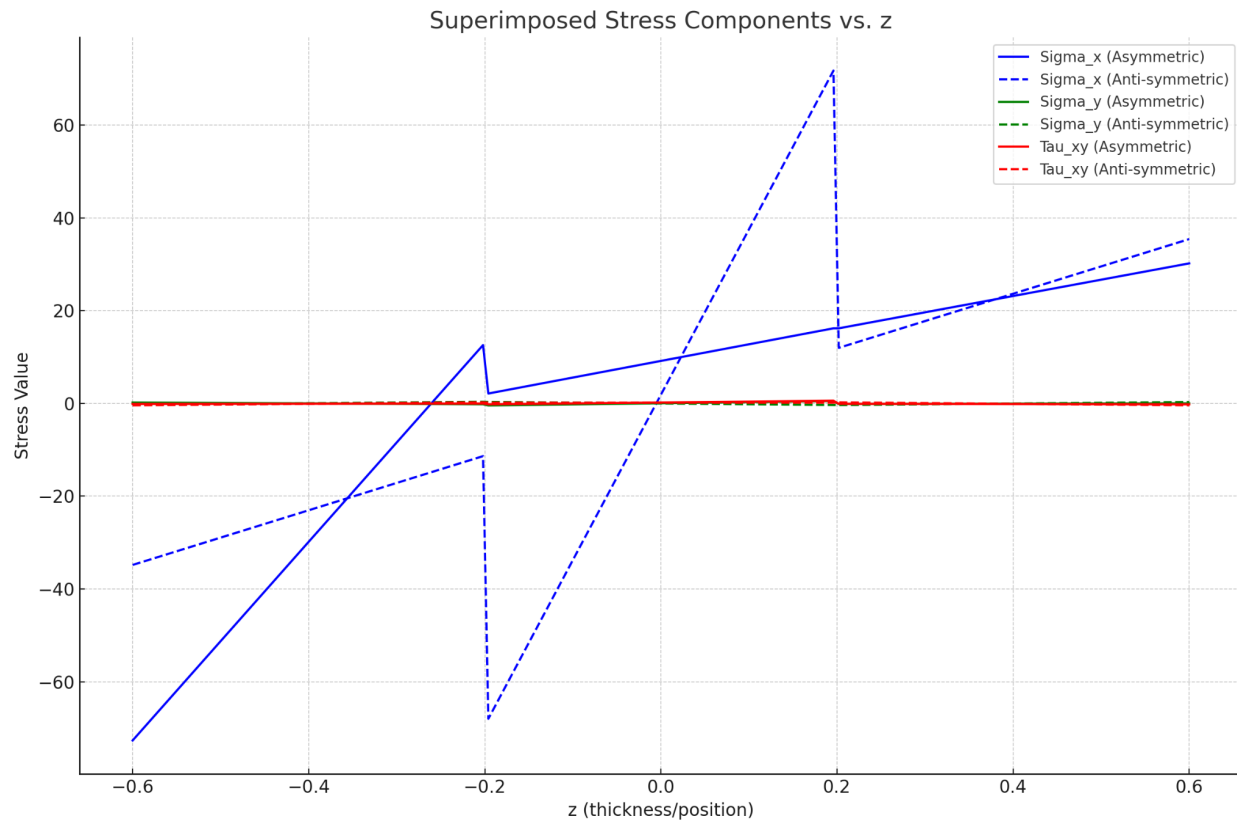


Fig 4.2.6: Superimposed Strain Components



**Fig 4.2.7: Superimposed Stress Components**

### 4.3: Validation [7]

---

The extensional stiffness matrix  $[A]$ , [kN/mm]

---

$$[A] = \begin{bmatrix} 31.25 & 9.94 & 0 \\ 9.94 & 31.25 & 0 \\ 0 & 0 & 10.65 \end{bmatrix}$$


---

**Fig 4.3.1: Validation for A Matrix**

The bending-stretching coupling matrix  $[B]$ , [kN]

$$[B] = \begin{bmatrix} 0 & 0 & -1.53 \\ 0 & 0 & -4.6 \\ -1.53 & -4.6 & 0 \end{bmatrix} \quad [B] = \begin{bmatrix} -6.64 & 1.33 & -0.76 \\ 1.33 & 3.97 & -2.3 \\ -0.76 & -2.3 & 1.33 \end{bmatrix}$$

The bending stiffness matrix  $[D]$ , [kN·mm]

$$[D] = \begin{bmatrix} 1.98 & 1.55 & 0 \\ 1.55 & 4.81 & 0 \\ 0 & 0 & 1.63 \end{bmatrix} \quad [D] = \begin{bmatrix} 4.63 & 1.02 & -0.31 \\ 1.02 & 3.22 & -0.92 \\ -0.31 & -0.92 & 1.10 \end{bmatrix}$$

**Fig 4.3.2: Validation for B & D Matrices [7]**

Strains  $(\varepsilon_x, \varepsilon_y, \gamma_{xy})$  and distribution of strains on laminate thickness

$[+ 60/0/-60]$		$\varepsilon_x$	$\varepsilon_y$	$\gamma_{xy}$	$[0/\pm 60]$		$\varepsilon_x$	$\varepsilon_y$	$\gamma_{xy}$
$i = 1$	sup.	-4.014	1.265	0.048	$i = 1$	sup.	-1.375	0.417	-0.035
	inf.	-1.314	0.414	0.049		inf.	0.247	-0.09	-0.006
$i = 2$	sup.				$i = 2$	sup.	1.058	-0.343	0.008
	$z = 0$	0.036	-0.011	0.049		$z=0$	1.058	-0.343	0.008
$i = 3$	inf.	1.386	-0.436	0.049	$i = 3$	inf.	1.869	-0.596	0.023
	sup.					sup.	3.491	-1.103	0.051
$i = 3$	inf.	4.086	-1.287	0.05		inf.			

**Fig 4.3.3: Validation for Strain Distribution [7]**

Stresses  $(\sigma_x, \sigma_y, \tau_{xy})$  and distribution of stresses on laminate thickness, [kN/mm<sup>2</sup>]

$[+ 60/0/-60]$		$\sigma_x$	$\sigma_y$	$\tau_{xy}$	$[0/\pm 60]$		$\sigma_x$	$\sigma_y$	$\tau_{xy}$
$i = 1$	sup.	-34.808	-0.305	-0.406	$i = 1$	sup.	-72.682	0.184	-0.117
	inf.	-11.235	0.382	0.254		inf.	13.015	-0.175	-0.021
$i = 2$	sup.	-69.413	0.328	0.162	$i = 2$	sup.	1.993	-0.44	-0.186
	$z = 0$	1.903	-0.006	0.163		$z=0$	9.166	0.046	0.209
$i = 3$	inf.	73.219	-0.34	0.165	$i = 3$	inf.	16.339	0.532	0.604
	sup.	11.866	-0.354	0.238		sup.	16.124	0.116	-0.078
$i = 3$	inf.	35.431	0.306	-0.4		inf.	30.195	0.028	-0.197

**Fig 4.3.4: Validation for Stress Distribution**

## **4.4: Social Implications**

### **Contribution to Safer and Lighter Structures**

The study of quasi-isotropic composite laminates, particularly those reinforced with S-glass fiber, aims to improve mechanical strength while reducing structural weight. In real-life applications such as automobiles, wind turbine blades, and infrastructure panels, these materials can reduce the risk of mechanical failure, increase energy efficiency, and improve public safety.

### **Promotion of Cost-Effective Manufacturing**

The chosen hand lay-up fabrication method is simple, low-cost, and does not require high-end equipment. This makes it suitable for small and medium-sized industries and local workshops, especially in developing regions. It helps democratize access to advanced composite manufacturing, reducing dependency on costly imports.[34]

### **Technical Skill Development**

The hands-on nature of the fabrication and testing process (including tensile and bending tests) offers excellent opportunities for practical engineering training. Students and technicians engaged in such projects gain valuable experience in composite design, mechanical analysis, and experimental methods—skills highly valued in industrial and academic sectors.[33]

#### **Support for Local Industry and Employment**

By simplifying the material selection (S-glass and polyester) and fabrication method, this research creates opportunities for small-scale production units and local startups to engage in composite manufacturing. This contributes to job creation, enhances technical capacity, and can support economic growth in emerging markets.[35]

#### **Advancement of Applied Engineering Education**

This project connects academic theory with practical experimentation, encouraging interdisciplinary learning and innovation. It supports national goals of enhancing applied research, encouraging innovation, and building engineering capacity among the next generation of professionals.[36]

### **4.5: Sustainability and Environmental Implications**

#### **Energy-Efficient Fabrication Process**

The hand lay-up process used in this study involves room-temperature curing, which significantly reduces the energy demand compared to oven- or autoclave-based curing. No external heat or pressure was applied during fabrication, making it a low-carbon, low-energy process.

## **Optimized Use of Raw Materials**

A fiber volume fraction of 60% was targeted to reduce excess polyester resin usage while maintaining mechanical integrity. The use of varied GSM values (200, 400, 600 gsm) and intelligent stacking sequences ensures that the composite performance is optimized with minimal material waste.

## **Acknowledgment of Environmental Limitations**

While polyester resin is not biodegradable and emits VOCs during curing, the study acknowledges these drawbacks. The aim is to optimize design and usage so that material efficiency offsets environmental harm. This also opens the door for future research into more sustainable resin systems.

## **Pathway to Greener Alternatives**

The testing and validation conducted in this project create a baseline for future comparison with bio-based resins, thermoplastic recyclable matrices, or natural fiber composites. These findings can guide environmentally conscious decision-making in both academia and industry.

## **Encouragement of Eco-Conscious Design Thinking**

By emphasizing laminate design efficiency—such as through stacking orientation—the project supports the principle of "designing smarter to use fewer resources." It contributes to a mindset where performance is enhanced not just by material choice but by structural logic.

#### **Local and Scalable Sustainable Solutions**

Since the process uses basic tools and accessible materials, it can be scaled in environmentally conscious ways even in low-resource environments. This supports community-based sustainable engineering, especially in rural or developing areas.

## 4.6: Limitations of the Thesis

1. **Limited Range of Stacking Sequences:** Only two quasi-isotropic stacking sequences — anti-symmetric  $[+60/0/-60]$  and asymmetric  $[0/+60/-60]$  were investigated. Other potentially significant configurations, such as symmetric or angle-ply layups, were not considered.
2. **Restricted GSM Variants:** The study focused on only two GSM values: 200 gsm and 600 gsm. Intermediate GSMS ( 300, 400 gsm) were not evaluated, which may have provided smoother trends and optimization points.
3. **Manual Fabrication Method:** The hand lay-up method was used without vacuum or pressure-assisted techniques. This may have led to inconsistencies such as air entrapment, uneven resin distribution, or laminate thickness variation.
4. **Single Matrix Material:** Only polyester resin was used as the matrix. Performance differences due to alternative matrices like epoxy, vinyl ester, or bio-resins were not explored.
5. **Mechanical Testing Scope:** The experimental analysis was limited to tensile and bending (flexural) tests. Other important mechanical properties, such as impact strength, fatigue

life, and interlaminar shear strength, were not evaluated.

6. **Environmental and Durability Aspects Not Studied:** The effects of moisture, temperature, UV exposure, or long-term aging were not considered. These factors could significantly influence the mechanical performance of composites in real-world applications.
7. **Small Sample Size for Each Configuration:** A limited number of samples were tested for each configuration, which may affect the statistical robustness of the results and conclusions.
8. **Manual Cutting Due to Safety Constraints:** The composite laminates could not be cut using laser or 3D printing-based methods, as the heat generated poses a fire hazard due to the flammability of the polyester resin. As a result, all specimens were cut manually using hand-operated tools, which may introduce slight dimensional inconsistencies and edge imperfections.
9. **Brush Used Instead of Resin Roller:** Due to equipment limitations, resin application during fabrication was performed using a brush instead of a resin roller, which is typically more effective in ensuring uniform resin distribution and better fiber wet-out. This may have resulted in uneven resin content, local dry spots, or trapped air within the laminate.

**10. Possible Misalignment During Fiber Placement:** During manual lay-up, individual fiber strands may have shifted or deviated from their intended orientation while being placed on the baseboard. This unintentional misalignment could impact the consistency of fiber direction, affecting the overall accuracy and repeatability of the mechanical properties.

11. For analytical analysis, the GSM of S-glass fiber was unknown.
12. The simulation results only gave tensile and compressive, stress and strain.

Other key properties were unknown

# Chapter 5

## CONCLUSIONS AND RECOMMENDATIONS

---

### 5.1: Conclusion

This study investigated the mechanical properties of S-glass fiber/polyester composite laminates, focusing on the effects of stacking sequence and areal weight (GSM) on their tensile and flexural performance. Two different stacking sequences, namely anti-symmetric  $[+60^\circ/0^\circ/-60^\circ]$  and asymmetric  $[0^\circ/+60^\circ/-60^\circ]$ , were explored with fiber areal weights of 200 gsm and 600 gsm.

The results demonstrated that the stacking sequence and GSM significantly influence the mechanical properties of the composite laminates. The  $[+60^\circ/0^\circ/-60^\circ]$  anti-symmetric laminate configuration consistently outperformed the  $[0^\circ/+60^\circ/-60^\circ]$  asymmetric laminate in terms of both bending strength and flexural modulus when tested with 200 gsm S-glass fiber. This behavior can be attributed to the balanced and symmetric fiber orientation, which results in better stress distribution and superior mechanical performance. Conversely, the 600 gsm laminates showed improved tensile strength compared to their 200 gsm counterparts, suggesting the role of higher fiber content in enhancing load-bearing capacity.

For flexural performance, the 600 gsm laminate with the  $[0^\circ/+60^\circ/-60^\circ]$  asymmetric stacking sequence demonstrated a better balance of mechanical properties, offering higher flexural stiffness and tensile properties. This finding emphasizes the importance of selecting the appropriate GSM based on the intended application, where the choice between 200 gsm and 600 gsm hinges on specific performance requirements such as stiffness or tensile strength.

The experimental data were validated using Classical Lamination Theory (CLT), and the findings were consistent with the predictions, confirming the reliability of the analytical approach. This research provides a deeper understanding of the influence of stacking sequence and GSM on the mechanical behavior of composite laminates, thus offering valuable insights for the design and optimization of high-performance composite materials in engineering applications.

## **5.2: Recommendations**

**Future Research on Hybrid Composites:** Further studies should explore the use of hybrid laminates incorporating both 200 gsm and 600 gsm fibers within the same laminate. This could provide a more efficient use of materials while optimizing mechanical performance for cost-effective applications.

**Broader Range of Stacking Sequences:** Additional research should consider a broader spectrum of stacking sequences, such as symmetric and angle-ply configurations, to evaluate their effects on the composite's anisotropic behavior. This would allow for a more comprehensive understanding of how different fiber orientations influence composite performance.

**Impact and Fatigue Testing:** This research focused on tensile and flexural testing, but other mechanical properties such as impact resistance, fatigue life, and interlaminar shear strength should be investigated in future studies to provide a more complete assessment of the laminate's overall performance under dynamic loading conditions.

**Environmental Effects:** It is recommended that future research explore the long-term effects of environmental factors, such as moisture absorption, UV exposure, and thermal aging, on the

mechanical properties of S-glass/polyester composite laminates. These factors are crucial for assessing the durability and service life of composite materials in real-world applications.

**Alternative Matrix Materials:** Further studies should also evaluate the use of alternative matrix materials, such as epoxy resins or bio-based polymers, to explore their impact on the composite's mechanical performance and sustainability.

## REFERENCES

---

- [1] R. Hanson Jimit, K. Ariffin Zakaria, O. Bapokutty, and S. Dhar Malingam, “Tensile and fatigue behaviour of glass fibre reinforced polyester composites,” International Journal of Engineering & Technology, vol. 7, no. 3.17, pp. 25–27, Aug. 2018.  
<https://doi.org/10.14419/ijet.v7i3.17.16615>
- [2] M. T. Alam, M. A. H. Akhand, and M. R. A. Kadir, “Mechanical properties of glass fiber reinforced polyester composites,”
- [3] A. Z. Rizvi, M. Asim, M. Jawaid, and M. T. H. Sultan, “Tensile, flexural, and impact performance of glass fiber-reinforced polyester composites: Effect of fiber surface treatment,” Composites Communications, vol. 38, p. 101655, 2023.
- [4] R. Kumar and D. Das, “A study on mechanical behavior of fiber reinforced polyester composites,” Asian Journal of Applied Science and Technology (AJAST), vol. X, no. Y, pp. Z-ZZ, YEAR.
- [5] B. Panchal, “Classical Laminate Theory (CLT) and its use for designing and manufacturing of FRP plates,”
- [6] M. A. M. Ali, Analysis of Mechanical Properties of Glass Fiber Reinforced Polymer Composites Using Classical Laminate Theory, M.S. thesis,

- [7] D. Hudișteanu and N. Țăranu, “The influence of the stacking sequence on stress and strain distributions for quasi-isotropic laminates,” *Bulletin of the Polytechnic Institute of Iași, Constructions. Architecture Section*, vol. 61, no. 2, pp. 97–110, 2015.
- [8] ASTM International, Standard Test Method for Tensile Properties of Plastics, ASTM D638–14, West Conshohocken, PA, USA, 2014.
- [9] M. S. M. Jusoh, M. A. N. Mohd Shukry, M. S. Abdul Majid, and M. R. Ishak, “Influence of stacking sequence on mechanical and dynamic mechanical properties of glass fiber reinforced polyester composites,” *Materials Research*, vol. 19, no. 6, pp. 1270–1278, Nov./Dec. 2016. doi: 10.1590/1980-5373-mr-2016-0397.
- [10] R. C. N. Oliveira, M. R. Silva, and A. S. Silva, “Effect of stacking sequence on mechanical properties of S-glass fiber reinforced polyester composites,” *Composite Structures*, vol. 200, pp. 750–757, Jan. 2018. doi: 10.1016/j.compstruct.2018.05.012.
- [11] A. F. Abd Ghani and J. Mahmud, “Characterisation of hybrid carbon glass fiber reinforced polymer (C/GFRP) of balanced cross ply and quasi isotropic under tensile and flexural loading,” *International Journal of Automotive and Mechanical Engineering*, vol. 17, no. 1, pp. 7792–7804, 2020. doi: 10.15282/ijame.17.1.2020.18.0582.
- [12] M. S. M. Jusoh, M. A. N. Mohd Shukry, M. S. Abdul Majid, and M. R. Ishak, “Influence of stacking sequence on mechanical and dynamic mechanical properties of glass fiber reinforced polyester composites,” *Materials Research*, vol. 19, no. 6, pp. 1270–1278, Nov./Dec. 2016. doi: 10.1590/1980-5373-mr-2016-0397.

- [13] M. A. S. Kamal, M. A. N. Mohd Shukry, and M. S. M. Jusoh, “Effect of stacking sequence and fiber volume fraction on mechanical behavior of quasi-isotropic glass fiber reinforced polymer composites,” *Composite Structures*, vol. 206, pp. 578–588, Apr. 2019. doi: 10.1016/j.compstruct.2018.09.045.
- [14] M. M. Rahman, M. R. Islam, and S. M. Sapuan, “Mechanical properties and failure analysis of S-glass fiber reinforced polymer composite laminates,” *Journal of Composite Materials*, vol. 54, no. 14, pp. 1959–1971, May 2020. doi: 10.1177/0021998320923234.
- [15] A. R. Bunsell and J. Renard, *Fundamentals of Fibre Reinforced Composite Materials*, 2nd ed. Boca Raton, FL, USA: CRC Press, 2005, pp. 87–89.
- [16] Beihai Fiberglass, “S-glass fiber high strength product,” FiberglassFiber.com, 2024.
- [17] “Resins – Discover Composites,” DiscoverComposites.com, 2025.
- [18] O. Chika O. Ujah and P. Popoola, “Gel time prediction of polyester resin for lamination of polymer composites,” *Bull. Chem. Soc. Ethiop.*, vol. 34, no. 2, pp. 235–245, May 2020.
- [19] M. P. Silva, P. Santos, J. M. Parente, S. Valvez, P. N. B. Reis, and A. P. Piedade, “Effect of post-cure on the static and viscoelastic properties of a polyester resin,” *Polymers*, vol. 12, no. 9, art. 1927, Sep. 2020, doi: 10.3390/polym12091927.
- [20] A. Ariman, E. Yalçınöz, and B. Aslan, “Investigation of mechanical properties of glass fiber reinforced composites,” \*International Research Journal of Engineering and Technology (IRJET)\*, vol. 8, no. 5, pp. 2274–2280, May 2021.

- [21] C. T. Herakovich, "Stress distribution," in Mechanics of Fibrous Composites. New York, NY, USA: John Wiley & Sons, Inc., 1998, pp. 145-158.
- [22] R. M. Jones, "Classical Lamination Theory," in Mechanics of Composite Materials, 2nd ed. Philadelphia, PA, USA: Taylor & Francis, 1999, pp. 190–195
- [23] P. Prasad, S. Kumar, and N. Shastry, "Fabrication and characterization of tensile properties of laminated composites – effect of fiber orientation," *Int. J. Eng. Res. Technol.*, vol. 2, no. 9, pp. 123–130, Sep. 2013.
- [24] Y. Xia et al., "Long chopped glass fiber reinforced low-density unsaturated polyester resin under different initiation," *Materials*, vol. 14, no. 23, Art. no. 7307, 2021.  
<https://doi.org/10.3390/ma14237307>
- [25] H. Plough, J. Wagoner, A. Hossain, and M. Kharshiduzzaman, "Effects of Lamina Stacking Sequence (LSS) on Composite Strength,"
- [26] P. N. B. Reis, P. S. Alves, J. M. Pina, S. Vaz, A. P. Piedade, and M. P. Soares, "Effect of post-cure on the static and viscoelastic properties of a polyester resin," *Polymers*, vol. 12, no. 9, Art. no. 1927, pp. 1–13, Sep. 2020.
- [27] A. Nugroho, K. Abdurohman, Kusmono, H. Hestiawan, and Jamasri, "Effect of manufacturing method to tensile properties of hybrid composite reinforced by natural (Agel Leaf Fiber) and glass fibers," in *Journal of Physics: Conference Series*, vol. 1005, 1st Int. Seminar Aerosp. Sci. & Technol., Yogyakarta, Indonesia, Dec. 2018, Art. no. 012004, pp. 1–6.
- [28] E. T. Abdullah, "A study of bending properties of unsaturated polyester/glass fiber reinforced composites," *J. Al-Nahrain Univ. Sci.*, vol. 16, no. 3, pp. 129–132, 2013.

- [29] M. Vaziri and M. Ashoory, "Using MATLAB to Design and Analyse Composite Laminates," Open Journal of Composite Materials, vol. 8, no. 1, pp. 1-9, 2018.
- [30] J. N. Reddy, Mechanics of Laminated Composite Plates and Shells: Theory and Analysis, 2nd ed. Boca Raton, FL, USA: CRC Press, 2004.
- [31] S. K. Bhudolia, P. D. Pore, and M. Y. Patil, "Flexural behavior of glass fiber reinforced polyester composites," \*Materials Today: Proceedings\*, vol. 4, no. 8, pp. 7821–7826, 2017.
- [32] M. K. Surappa and B. N. Reddy, "Tensile properties of glass fiber reinforced polyester composites," Materials Science and Engineering: A, vol. 528, no. 18, pp. 5963–5970, 2011.
- [33] Shashitha C. Kularatna, "Developments in advanced composites skills training and manufacturing through Virtual Reality and an Artificially Intelligent Layup Agent," Ph.D. dissertation, Bristol Composites Institute, Univ. of Bristol, UK, 2019.
- [34] F. Cucinotta, E. Guglielmino, and F. Sfravara, "Life cycle assessment in yacht industry: A case study of comparison between hand-lay-up and vacuum infusion," J. Clean. Prod., vol. 142, pp. 123–130, Oct. 2016.
- [35] C. Ghafafian and S. Nutt, "A multi-industry perspective to composite repairs," Appl. Composite Mater., Jun. 2025.
- [36] Composite materials and its advancements for a cleaner engine of future, Composite Materials for Wind Power Turbine Blades, 2021.
- [37] Elsevier, "Classical Lamination Theory," in ScienceDirect Topics: Engineering, Elsevier B.V. Jun. 28, 20

# APPENDICES

## APPENDIX-A

---

### Code for the Optimization Program

(Software Used: Matlab)

#### Matlab Command

##### 1. For A, B and D matrices

```
%% 1. Material properties  
Ef = 85.5; Em = 4.0;    % GPa  
Gf = 26.72; Gm = 1.44;    % GPa  
vf = 0.22; vm = 0.39;  
Vf = 0.6; Vm = 1-Vf;  
  
E1 = Ef*Vf + Em*Vm;  
E2 = (Ef*Em)/(Ef*Vm + Em*Vf);  
G12 = (Gf*Gm)/(Gf*Vm + Gm*Vf);  
nu12 = vf*Vf + vm*Vm;  
nu21 = nu12*E2/E1;  
  
Q11 = E1/(1-nu12*nu21);  
Q22 = E2/(1-nu12*nu21);  
Q12 = nu12*E2/(1-nu12*nu21);
```

```

Q66 = G12;

Qred = [Q11 Q12 0; Q12 Q22 0; 0 0 Q66]; % kN/mm2

%% 2. Two stacking sequences

plyThk = 0.4; % mm

stacks(1).name = '[+60/0/-60] anti-sym';
stacks(1).angles = [ 60 0 -60];
stacks(2).name = '[0/+60/-60] asym';
stacks(2).angles = [ 0 60 -60];

for s = 1:2
    ang = stacks(s).angles;
    n = numel(ang);
    z = linspace(-n*plyThk/2, n*plyThk/2, n+1); % ply interfaces

    [A,B,D] = buildABD(Qred, ang, z);
    stacks(s).A = A; stacks(s).B = B; stacks(s).D = D;

    fprintf('\n==== %s ====\n', stacks(s).name);
    fprintf('[A] (kN/mm)\n'); disp(A);
    fprintf('[B] (kN)\n'); disp(B);
    fprintf('[D] (kN·mm)\n'); disp(D);
end

function [A,B,D] = buildABD(Qred,stack,z)
A = zeros(3); B = zeros(3); D = zeros(3);

```

```

for k = 1:numel(stack)

    Qb = QbarCS(Qred, stack(k));

    zk = z(k+1); zk1 = z(k);

    A = A + Qb*(zk - zk1);

    B = B + 0.5*Qb*(zk^2 - zk1^2);

    D = D + (1/3)*Qb*(zk^3 - zk1^3);

end

end

function Qb = QbarCS(Q,theta)

c = cosd(theta); s = sind(theta); c2=c^2; s2=s^2; c4=c2^2; s4=s2^2;

Q11=Q(1,1); Q22=Q(2,2); Q12=Q(1,2); Q66=Q(3,3);

Qb11 = Q11*c4 + 2*(Q12+2*Q66)*c2*s2 + Q22*s4;

Qb22 = Q11*s4 + 2*(Q12+2*Q66)*c2*s2 + Q22*c4;

Qb12 = (Q11+Q22-4*Q66)*c2*s2 + Q12*(c4+s4);

Qb66 = (Q11+Q22-2*Q12-2*Q66)*c2*s2 + Q66*(c4+s4);

Qb16 = (Q11-Q12-2*Q66)*c^3*s - (Q22-Q12-2*Q66)*c*s^3;

Qb26 = (Q11-Q12-2*Q66)*c*s^3 - (Q22-Q12-2*Q66)*c^3*s;

Qb = [Qb11 Qb12 Qb16; Qb12 Qb22 Qb26; Qb16 Qb26 Qb66];

end

```

## 2.Code For Strain and Stress Distribution on Laminate Thickness

```
%% 1. Material properties
```

```
Ef = 85.5; Em = 4.0; % GPa
```

```
Gf = 26.72; Gm = 1.44; % GPa
```

```
vf = 0.22; vm = 0.39;
```

```
Vf = 0.6; Vm = 1 - Vf;
```

```
E1 = Ef*Vf + Em*Vm;
```

```
E2 = (Ef*Em)/(Ef*Vm + Em*Vf);
```

```
G12 = (Gf*Gm)/(Gf*Vm + Gm*Vf);
```

```
nu12 = vf*Vf + vm*Vm;
```

```
nu21 = nu12 * E2 / E1;
```

```
Q11 = E1/(1 - nu12*nu21);
```

```
Q22 = E2/(1 - nu12*nu21);
```

```
Q12 = nu12*E2/(1 - nu12*nu21);
```

```
Q66 = G12;
```

```
Qred = [Q11 Q12 0; Q12 Q22 0; 0 0 Q66]; % kN/mm2
```

```
%% 2. Stack definitions
```

```
plyThk = 0.4;
```

```
stacks(1).name = '[+60/0/-60] Anti-symmetric';
```

```
stacks(1).angles = [ 60 0 -60];
```

```

stacks(2).name = '[0/+60/-60] Asymmetric';

stacks(2).angles = [ 0 60 -60];

%% 3. Loop through both stacks

for s = 1:2

    ang = stacks(s).angles;
    n = numel(ang);
    z = linspace(-n*plyThk/2, n*plyThk/2, n+1);

    [A,B,D] = buildABD(Qred, ang, z);
    ABD = [A B; B D];

    stacks(s).A = A; stacks(s).B = B; stacks(s).D = D;

    % Apply in-plane & bending loads

    N = [1; 0; 0]; % kN/mm
    M = [10; 0; 0]; % kN·mm/mm
    loadVec = [N; M];
    x = ABD \ loadVec;
    eps0 = x(1:3); kappa = x(4:6);

    % Stress and strain through thickness

    zEval = linspace(z(1), z(end), 200);
    strainZ = zeros(3,numel(zEval));
    stressZ = zeros(3,numel(zEval));

    for j = 1:numel(zEval)

```

```

zj = zEval(j);

strain = eps0 + zj * kappa;

ply = find(z(1:end-1) <= zj & z(2:end) >= zj, 1);

Qbar = QbarCS(Qred, ang(ply));

stress = Qbar * strain;

strainZ(:,j) = strain;

stressZ(:,j) = stress;

end

% Store for plotting

stacks(s).zEval = zEval;

stacks(s).strainZ = strainZ;

stacks(s).stressZ = stressZ;

end

%% 4. Plotting

for s = 1:2

zEval = stacks(s).zEval;

strainZ = stacks(s).strainZ;

stressZ = stacks(s).stressZ;

figure('Name', ['Strain - ' stacks(s).name]);

plot(strainZ(1,:),zEval,'r', strainZ(2,:),zEval,'g', strainZ(3,:),zEval,'b');

xlabel('Strain'); ylabel('z (mm)'); grid on;

legend('\epsilon_x','\epsilon_y','\gamma_xy');

title(['Mid-plane Strain Distribution: ' stacks(s).name]);

```

```

figure('Name', ['Stress - ' stacks(s).name]);
plot(stressZ(1,:),zEval,'r', stressZ(2,:),zEval,'g', stressZ(3,:),zEval,'b');
xlabel('Stress (kN/mm2)'; ylabel('z (mm)'); grid on;
legend('\sigma_x','\sigma_y','\tau_{xy}');
title(['Stress Distribution: ' stacks(s).name]);

end

%% 5. Export CSV

for s = 1:2

    writematrix([stacks(s).zEval.' stacks(s).strainZ.], ['strain_ ' sName(stack(s).name) '.csv']);
    writematrix([stacks(s).zEval.' stacks(s).stressZ.], ['stress_ ' sName(stack(s).name) '.csv']);

end

function Qb = QbarCS(Q,theta)

c = cosd(theta); s = sind(theta); c2=c^2; s2=s^2; c4=c2^2; s4=s2^2;

Q11=Q(1,1); Q22=Q(2,2); Q12=Q(1,2); Q66=Q(3,3);

Qb11 = Q11*c4 + 2*(Q12+2*Q66)*c2*s2 + Q22*s4;

Qb22 = Q11*s4 + 2*(Q12+2*Q66)*c2*s2 + Q22*c4;

Qb12 = (Q11+Q22-4*Q66)*c2*s2 + Q12*(c4+s4);

Qb66 = (Q11+Q22-2*Q12-2*Q66)*c2*s2 + Q66*(c4+s4);

Qb16 = (Q11-Q12-2*Q66)*c^3*s - (Q22-Q12-2*Q66)*c*s^3;

Qb26 = (Q11-Q12-2*Q66)*c*s^3 - (Q22-Q12-2*Q66)*c^3*s;

Qb = [Qb11 Qb12 Qb16; Qb12 Qb22 Qb26; Qb16 Qb26 Qb66];

end

function [A,B,D] = buildABD(Qred,angles,z)

A = zeros(3); B = zeros(3); D = zeros(3);

```

```

for k = 1:numel(angles)

    Qb = QbarCS(Qred, angles(k));

    zk = z(k+1); zk1 = z(k);

    A = A + Qb*(zk - zk1);

    B = B + 0.5*Qb*(zk^2 - zk1^2);

    D = D + (1/3)*Qb*(zk^3 - zk1^3);

end

end

function tag = sName(name)

tag = lower(regprep(name,'[^a-zA-Z0-9]','_'));

end

```

